

GEOARCHAEOLOGICAL INVESTIGATION OF THE COATS-HINES SITE
(40WM31), WILLIAMSON COUNTY, TENNESSEE

A Thesis

by

KAYLA ANNE SCHMALLE

Submitted to the Office of Graduate Studies of
Texas A&M University
in partial fulfillment of the requirements for the degree of

MASTER OF ARTS

Chair of Committee,	Michael R. Waters
Committee Members,	Ted Goebel
	Cristine L.S. Morgan
Head of Department,	Cynthia Werner

August 2013

Major Subject: Anthropology

Copyright 2013 Kayla Anne Schmalte

ABSTRACT

The Coats-Hines site (40WM31) is a potential pre-Clovis site located in Franklin, Tennessee. The site rests, geographically, at the convergence of the Central Basin and Western Highland Rim. The site was discovered during the construction of a nearby golf course when a salvage team uncovered a mature female mastodon.. The site was later excavated in 1994-1995, during which time two additional mastodons were uncovered, in direct association with lithic artifacts. Preliminary radiocarbon dates reveal the site was deposited during the late Pleistocene epoch at roughly 12,000 ^{14}C yr BP.

During the summer of 2012, the site was excavated with the goal of determining the depositional setting of the site and geographic region, as well as establishing the antiquity of the archaeological remains. The site geology was determined through field interpretation and texturing, micromorphological analysis, laboratory particle size analysis, and radiocarbon dating. Sedimentation at the site is a combination of cherty colluvium from upslope as well as alluvium. Four chronostratigraphic sequences of sedimentation were determined to have occurred during the last glacial, the Pleistocene-Holocene transition, the Holocene, and modern time periods. The volume, distribution, and composition of the nine defined stratigraphic units are dependent on the fluctuations occurring in the climate during these time periods. The climate changes and rates of deposition occurring at Coats-Hines were correlated to similar sites in the region.

The Coats-Hines site was surveyed along the wet-weather drainage that bounds the site during in the spring of 2013. A channel unconformity was discovered, likely

dating to the Pleistocene-Holocene transition and providing context to the 1994/1995 excavation.

DEDICATION

This thesis is dedicated to my parents, Verlynn and Anne Schmalle, who have supported me unconditionally every step of the way.

ACKNOWLEDGEMENTS

I would like to thank my committee chair, Dr. Michael Waters, for giving me the opportunity to work at the Coats-Hines site and develop this project; his support and guidance in the field, as well as during the laboratory analysis and writing process made this thesis possible. I would also like to thank Dr. Ted Goebel for his invaluable advice and support throughout my time at Texas A&M. Thanks to Dr. Cristine Morgan, for her instruction and patience throughout the course of this research.

I would like to thank Roy J. Shlemon, the Center for the Study of the First Americans, and Department of Anthropology at Texas A&M for their financial support, making this research possible. In addition, I would like to thank Paul and Sharlene Litchy, for allowing myself and Texas A&M to conduct the survey and excavation on their property.

I thank John Broster and Mark Norton for their expertise on the Coats-Hines site and spending time out at the site during the summer of 2012. Thanks also go to Dr. Steven Driese, for taking the time to analyze thin sections, and providing his expert opinion and interpretation. Thanks to Dr. Randy Cox, for helping to figure out a geologic puzzle that had me baffled for months. And a special thanks to Donna Prochaska for having the patience to help me in the Soil Characterization Lab.

I want to extend my gratitude to my friends, Courtney Cox and Stephanie Stutts for their hard work in the field, spending long nights organizing the excavation. I would like to thank my friend and fellow graduate student, Angela Gore, for devoting an entire

week surveying the site, I literally would not have been able to do it without you. Thanks also to Joshua Keene for his technical support and valuable advice.

Thanks to my parents, Anne and Verlynn Schmalle for their encouragement, for keeping me focused, and for keeping the lights on. Thanks to my sister, Greta Schmalle, for showing me the ropes of being a successful graduate student.

TABLE OF CONTENTS

	Page
ABSTRACT.....	ii
DEDICATION.....	iv
ACKNOWLEDGEMENTS.....	v
TABLE OF CONTENTS.....	vii
LIST OF FIGURES.....	ix
LIST OF TABLES.....	xi
CHAPTER I INTRODUCTION AND PROJECT OUTLINES.....	1
1.1 Introduction.....	1
1.2 Project Outline 2012/2013.....	2
CHAPTER II BACKGROUND.....	6
2.1 Background to the Coats-Hines Site (40WM31).....	6
2.2 Radiocarbon (¹⁴ C) Dates from Past Excavations.....	12
CHAPTER III PHYSIOGRAPHIC SETTING.....	13
3.1 Topography.....	13
3.2 Bedrock.....	15
3.3 Modern Climate.....	16
CHAPTER IV GEOLOGY.....	17
4.1 Introduction.....	17
4.2 2012 Excavation Area.....	20
4.3 Macromorphology: Turbation Features.....	23
4.4 Micromorphological Analysis.....	26
4.4.1 Introduction to Micromorphology.....	26
4.4.2 Methods of Micromorphological Analysis.....	26
4.4.3 Interpretation of Micromorphological Thin Sections.....	28
4.5 Gravel Distribution.....	33

4.5.1 Introduction to Coarse Fragments.....	33
4.5.2 Methods of Gravel Analysis.....	34
4.5.3 Results of Gravel Analysis.....	36
4.5.3.1 Composition.....	36
4.5.3.2 Weight Distribution of Gravels.....	37
4.5.3.3 Roundness and Sphericity.....	39
4.5.3.4 Interpretation.....	41
4.6 Dates from the 2012 Excavation.....	41
4.7 Channel Unconformity.....	44
4.7.1 Introduction.....	44
4.7.2 Unit Descriptions.....	44
4.7.3 Interpretation.....	45
4.8 Geochronology.....	47
 CHAPTER V CORRELATIONS.....	 52
5.1 Introduction.....	52
5.2 The Duck River, Tennessee.....	53
5.3 The Pomme de Terre River, Missouri.....	53
5.4 Douthard Creek, West Virginia.....	54
5.5 Interpretation.....	55
 CHAPTER VI ARCHAEOLOGICAL CONTEXT.....	 58
6.1 Correlations of the 2012 Excavation to Previous Excavations at Coats- Hines.....	58
6.2 Context of Mastodon B.....	59
 CHAPTER VII CONCLUSION.....	 63
 REFERENCES.....	 65
 APPENDIX A.....	 68
 APPENDIX B.....	 69
 APPENDIX C.....	 70
 APPENDIX D.....	 74
 APPENDIX F.....	 78
 APPENDIX G.....	 79

LIST OF FIGURES

FIGURE		Page
1	Coats-Hines site map, including past excavations of the site.....	3
2	Adapted cross-section profile originally drawn by John Broster of Area B; geological descriptors were determined during the 1994 excavation also by John Broster.....	9
3	Summary of the locations of the stratigraphic profiles recorded during the 1994-1995, 2010, and 2012 excavations.....	9
4	Adapted 2010 test trench stratigraphic column drawn by Deter-Wolf et al. 2011. The representative proveniences of both the faunal and lithic remains are recorded within the column.....	11
5	Topographic map of the Coats-Hines site.....	14
6	Topographic relief of the Coats-Hines site area.....	14
7	Coats-Hines site 2012 excavation, east profile wall.....	18
8	Coats-Hines site 2012 excavation, north profile wall.....	19
9	Coats-Hines site 2012 excavation, south profile wall.....	19
10	Treethrow features along the east wall of the 2012 excavation pit.....	25
11	Manganese concretion, lateral illuvial clay coats in root pores, Unit 5, Sample 1, XPL, 1.25× magnification.....	30
12	Banded illuvial clay, Unit 5, Sample 1, PPL, 10 × magnification.....	31
13	Banded clay in root pore, depleted matrix, Unit 4, Sample 2, PPL, 10× magnification.....	31
14	Faecal pellets, Unit 4, Sample 2, PPL, 1.25 × magnification.....	32
15	Charcoal with cellular structure, Unit 2, Sample 4, XPL, 10× magnification.....	32

16	Iron Concretion with composite coating, Unit 1, Sample 7, PPL 4× magnification.....	33
17	Roundness and sphericity chart (Krumbein and Sloss 1963).....	36
18	Cumulative (Levels 51-61) composition of the gravel clasts in excavation levels 51-61 (Units 1-4).....	37
19	Total weight (g) of each excavation level of Unit N996/E1008 and their associated geologic unit.....	38
20	Roundness of gravels in excavation levels 51-61 of Unit N996/E1008. Presented using the average weight (%) of each roundness classification per level.....	40
21	Sphericity of gravels in excavation levels 51-61 of Unit N996/E1008. Presented using the percentage by volume of each sphericity classification by level.....	40
22	Generalized core of 2012 excavation units with associated radiocarbon dates (¹⁴ C yr BP).....	43
23	Locality I profile of channel unconformity.....	46
24	Locality II profile of channel unconformity.....	46
25	Generalized cross-section of the lithologic units at Coats-Hines.....	51
26	Study areas of the (1) Pomme de Terre River, Missouri; (2) Douthard Creek, West Virginia; (3) the Coats-Hines site, Tennessee; and (4) Duck River, Tennessee.....	52
27	Time correlations of deposition and stability between the Duck River, Pomme de Terre River, Coats-Hines site, and Douthard Creek.....	57
28	Planview of Mastodon B (Breitburg et al. 1996).....	60

LIST OF TABLES

TABLE		Page
1	Adapted table of radiocarbon dates from the 1994-1995 and 2010 excavations (Breitburg et al. 1996; Deter-Wolf et. al. 2011).....	12
2	Stratigraphic unit and micromorphological sample correlation.....	27
3	2012 radiocarbon dates.....	42
4	Correlation between the stratigraphic units of the 2010 and 2012 excavations.....	59

CHAPTER I

INTRODUCTION AND PROJECT OUTLINES

1.1 Introduction

The Coats-Hines site (40WM31) is located near the convergence of the Western Highland Rim and the Central Basin, in northern Williamson County, Tennessee (Breitburg and Broster 1995). The site was discovered in 1977 with the construction of a local golf course, uncovering mastodon (*Mammut americanum*) remains that would later be designated Mastodon A (Brietburg et al. 1996; Deter-Wolf et al. 2011). The salvage excavation that occurred in 1977 was never published and the site was not investigated further until a survey in 1994 by Emmanuel Brietburg and John Broster of the Tennessee Division of Archaeology (TDOA) (Brietburg et al. 1996). The TDOA discovered the remains of a second Mastodon eroding from the banks of a wet-weather drainage that bordered the site. An emergency excavation was completed by Breitburg and Broster in which the disarticulated remains of a young male mastodon were uncovered in association with several chert artifacts (Breitburg and Broster 1995). Initial radiocarbon dates for the 1994 mastodon (Mastodon B) yielded dates between $10,260 \pm 240$ ^{14}C yr BP and $12,030 \pm 40$ ^{14}C yr BP, which indicated that the Coats-Hines site was potentially a Clovis or pre-Clovis Paleoindian butchering site (Table 1) (Brietburg et al. 1996; Deter-Wolf et al. 2011).

In 2010 a test trench was excavated to validate the early radiocarbon dates obtained in 1994, as well as establish the location and distribution of archaeological remains at the site. The test trench yielded several Pleistocene bone fragments and a

radiocarbon date of $12,050 \pm 60$ ^{14}C yr BP, again placing the site in the pre-Clovis time range (Deter-Wolf et al. 2011) .

Although the Coats-Hines site has been excavated several times in the past, the stratigraphy, depositional history, and context of the archaeological and faunal remains have not been properly recorded. To propose a site of this potential antiquity and significance the data needs to be well-dated and provenienced. The site was again excavated during the Summer of 2012 by Texas A&M University to address the issues of context. The goal of this project specifically is to define the stratigraphy at the site using field and laboratory analysis, collect samples for radiocarbon dating to create a geochronological sequence, and establish the depositional history at the site. In addition, the remains of Mastodon B will be provenienced based on correlations to the established stratigraphy at the site and with lithological sequences in the region coinciding with climatic transitions occurring during the late Pleistocene-Holocene transition.

1.2 Project Outline 2012/2013

The 2012 Coats-Hines project excavated a 5 by 5 m excavation pit that intersected the corner of the 1994-1995 excavation along the north wall, and the 2010 test trench along the west (Figure 1). The excavation was later expanded along the west wall to include an additional 3 by 5 m of units. Each excavation unit was 1 by 1 m and excavated using 5 cm arbitrary levels within the stratigraphic units, beginning at a depth of up to 3 m below the ground surface. The datum elevation for the 2012 excavation was set at 99.914 m, which is not at the modern ground surface but is roughly at the

boundary between the 1994-1995 ground surface and its contact with the modern backfill of Unit 9.

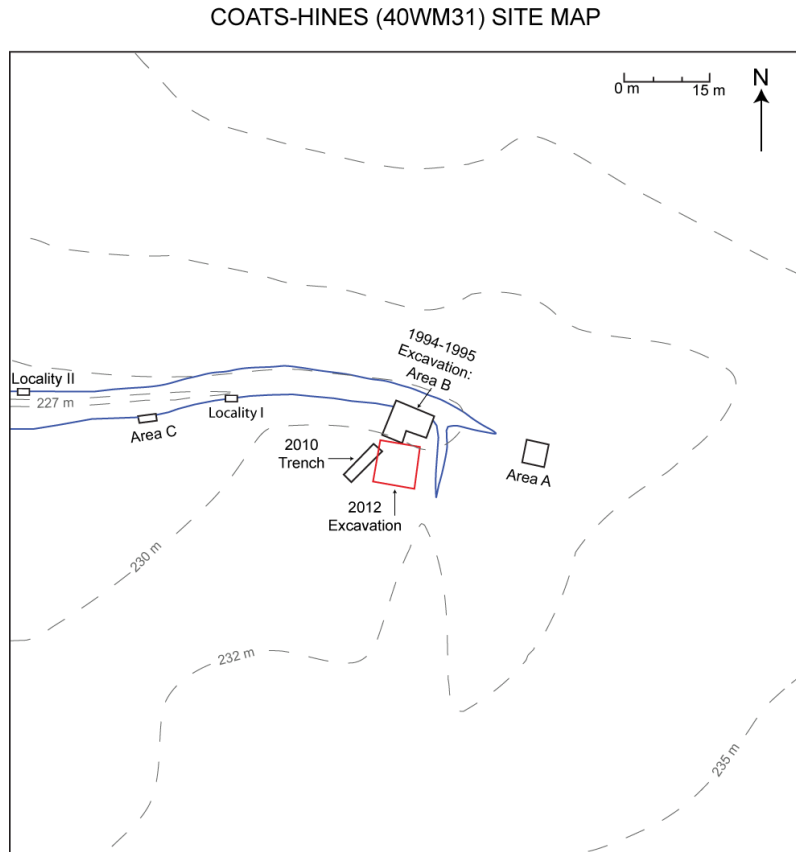


Figure 1. Coats-Hines site map, including past excavations of the site.

The 1994-1995 excavation as well as the 2010 trench were both discussed using depth from the modern ground surface. For ease of correlation, this study will also use depth from ground surface, but given the fluctuations in the modern ground surface elevation, especially following the 1994-1995 excavation when modern backfill covered the site stratigraphy, this study will also incorporate elevation in relation to the excavation datum.

Sediment within the excavation area was removed via bobcat to a depth of 1.5-1.6 m below the ground surface, or to a depth of 98.150-97.050 m. Following the removal of the overlying sediment, 5 cm levels were excavated with trowels beginning at excavation level 49 (98.050-98.00 m or 1.7 -1.75 m) up to excavation level 65 (97.25-97.2 m or 2.6-2.65 m). All sediment excavated from the 5 cm excavation levels was collected as a bulk sample and water screened.

The 2012 excavation area (Figure 1) was profiled based on field interpretation of the stratigraphic units. The sediment was later processed in the laboratory using the pipette method to determine the particle size distribution. In addition, micromorphological samples were collected for thin sectioning and analysis to determine soil formation processes, the structure of deformation features, and the general relatedness of each unit. Similarly, the coarse grained materials from the excavated levels were washed and analyzed to determine the source of colluvial/alluvial material, distance material was transported, and energy of deposition by unit. Finally, charcoal samples were collected from the excavation levels to create a geochronological sequence of deposition. The absence of charcoal above level 49 prevented the dating of the upper sequence of the 2012 excavation area, therefore the stratigraphic units of the upper profile are dated using relative dating methods and correlation to other regional stratigraphic profiles.

In March of 2013, the site was surveyed along the wet-weather drainage to determine the provenience, stratigraphy, and depositional history of a channel unconformity resting between what is believed to be Pleistocene and Holocene sediment

packages. The significance of the channel unconformity is related to the context of Mastodon B and will be discussed in later sections.

CHAPTER II

BACKGROUND

2.1 Background to the Coats-Hines Site (40WM31)

The Coats-Hines site (40WM31) is located near the western convergence of the Central Basin and the Highland Rim in northeast Williamson County and has been proposed as a potential pre-Clovis mastodon (*Mammut americanum*) butchering site (Breitburg et al. 1996; Deter-Wolf et al. 2011). The Coats-Hines site was first discovered in 1977 during the construction of a local golf course in northern Williamson County, Tennessee when several large bones were uncovered (Breitburg and Broster 1995; Breitburg et al. 1996; Deter-Wolf et al. 2011). A salvage excavation conducted by the Tennessee Division of Archaeology (TDOA) to recover the remains of what was discovered to be a partial mastodon skeleton (Breitburg and Broster 1995; Breitburg et al. 1996; Deter-Wolf et al. 2011). The skeletal remains of the mature, female mastodon were designated Mastodon A (Figure 1) (Deter-Wolf et al. 2011). Following the minimal excavation Area A was destroyed from construction and the analysis of the remains of Mastodon A were never published (Breitburg et al. 1996; Deter-Wolf et al. 2011).

A second mastodon was discovered when the TDOA returned to the area in the Spring of 1994 and surveyed the wet-weather drainage (Breitburg and Broster 1995; Breitburg et al. 1996). The TDOA discovered the backbone, ribs and tusk of a young male mastodon (*Mammut americanum*) eroding out of the south bank of the drainage (Breitburg and Broster 1995; Breitburg et al. 1996; Deter-Wolf et al. 2011). Following

the discovery of a second mastodon in the area, an emergency excavation was conducted by the TDOA in May of 1994 with the goal of collecting, mapping and removing soil, bone, and archaeological samples from the drainage for analysis (Breitburg and Broster 1995). The excavation area was designated Area B (Figure 1).

The 1994 excavation uncovered thirty-four chert specimens in direct association with the mastodon remains in Area B, including ten “formal” tools and twenty-four chert flakes (Breitburg et al. 1996; Deter-Wolf et al. 2011). The formal tools were defined as a prismatic blade fragment, a proximal bifacial knife, two graters, two unifacial side scrapers, and two cores (Breitburg et al. 1996). All thirty-four lithic artifacts are composed of locally-available Fort Payne chert, with the exception of one scraper and flake that is St. Louis chert, and one flake that is Dover chert (Breitburg et al. 1996; Deter-Wolf 2011).

Following the microscopic examination of the Area B mastodon, it was determined that cut marks were present on a thoracic vertebra, implicating that the Coats-Hines site is the first documented Paleoindian-mastodon site in Tennessee (Breitburg et al. 1996). In addition to the mastodon remains, the faunal complex of the 1994/1995 excavation includes skeletal elements of horse (*Equus* spp.), deer (*Odocoileus* sp.), muskrat (*Ondatra zibethicus*), turkey (*Meleagris gallopavo*) frog (*Rana* spp.) and turtle (*Chrysemys* cf.) (Breitburg et al. 1996).

The stratigraphy of the 1994-1995 excavation was recorded as a cross-section of the excavation across the drainages by John Broster of the TDOA (Figures 2 and 3). The late Pleistocene bone bed and lithic artifacts of the 1994-1995 excavations were recorded

as resting relatively level within blue/gray clay deposits, 2.1 m below the ground surface (Figure 2). Above the gleyed clay, John Broster recorded 70 cm of dark clay, with roughly 1.2 meters of brown loess capping the deposits (Figure 2). The late-Pleistocene deposits were described as being randomly mixed clays with slightly rounded chert cobbles. The stratigraphy of the site was stated to be compromised by the extensive disturbance of soil sediments by angle worms and tree-root growth, although the disturbance was not recorded in the cross-section profile of the excavation (Breitburg et al. 1996). Finally, the depositional environment of Area B was interpreted as an old stream channel, sinkhole, or beaver pond (Breitburg et al. 1996).

During the Spring of 1995, additional fragmentary mastodon remains were recorded eroding from the south bank of the drainage, to the west of Area B. The remains were designated Mastodon C and were recovered during the summer of 2008 (Figure 1) (Deter-Wolf et al. 2011). Mastodon C was discovered to be heavily fragmented, mineralized, and resting 1.5 m below the ground surface (Deter-Wolf et al. 2011).

COATS-HINES SITE (40WM31) 1995 AREA B: EAST WALL

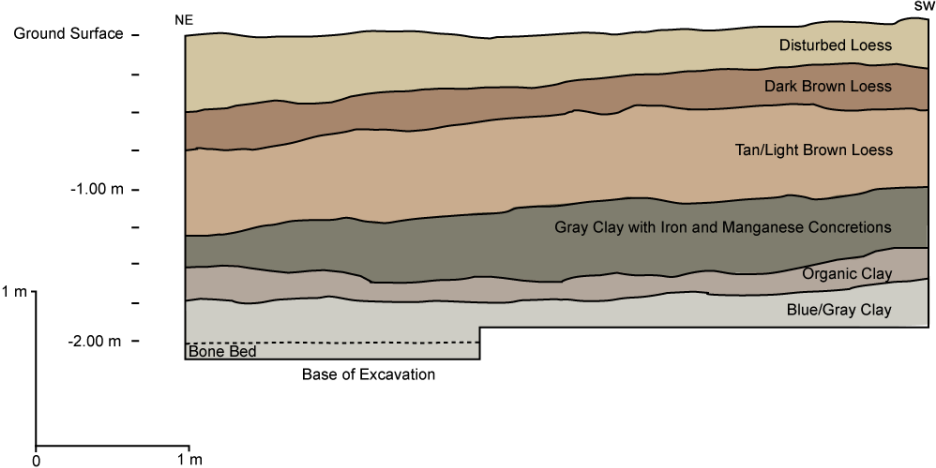


Figure 2. Adapted cross-section profile originally drawn by John Broster of Area B; geological descriptors were determined during the 1994 excavation also by John Broster.

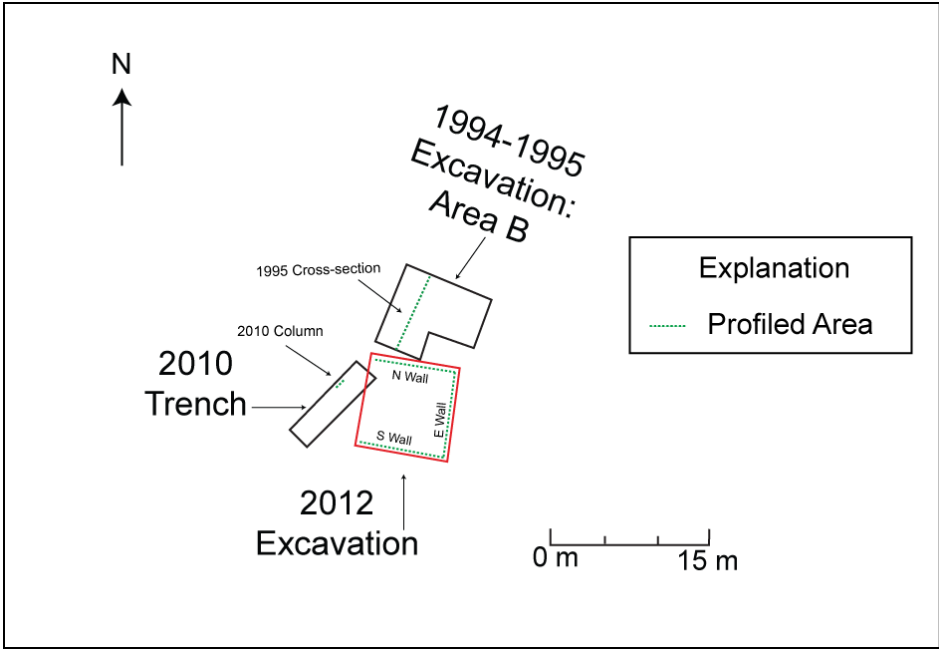


Figure 3. Summary of the locations of the stratigraphic profiles recorded during the 1994-1995, 2010, and 2012 excavations.

Finally, in 2010 the TDOA returned to the Coats-Hines site to conduct an archaeological test trench with the goal of determining the archaeological integrity/context of the Pleistocene deposits (Deter-Wolf et al. 2011). The trench was situated on a southwest to northeast diagonal, 4.5 m south of the wet-weather drainage (Figures 1 and 3) (Deter-Wolf et al. 2011). The TDOA uncovered 1,582 faunal elements consisting of mastodon, turtle, and rodent resting between 2.6 and 3.1 m below the ground surface (Deter-Wolf et al. 2011). In addition, ten lithic artifacts were recovered in situ between 2.6 and 2.8 m below the ground surface (Deter-Wolf et al. 2011).

During the 2010 excavation, five stratigraphic sediment packages were defined (Figures 3 and 4). The first, Unit Ia and Ib are defined as modern silt loam topsoil with rock fill and measures between 0 and roughly 1 m below the ground surface. The second unit, Unit IIa and IIb, is defined as a dark grayish brown (10YR 3/2) silt loam with a content of up to 50% manganese. Unit II rests between 1 and 1.8 m below the ground surface. Unit III is defined as a dark grayish brown (10YR 4/2) clay loam, measuring 1.8 to 2.1 m below the modern ground surface. Unit IV is a dark gray (10YR 4/1) mottled clay loam between 2.1 and 2.3 m below the ground surface (Deter-Wolf et al. 2011). Finally, Unit V is a grayish brown (10YR 5/2) mottled clay with up to 50% manganese content, measuring 2.3 to 3.5 m below the modern ground surface (Deter-Wolf et al. 2011). Unit V is also the unit that contained the lithic artifacts and Pleistocene bone fragments (Figure 4).

COATS-HINES (40WM31) 2010 TEST TRENCH STRATIGRAPHIC COLUMN

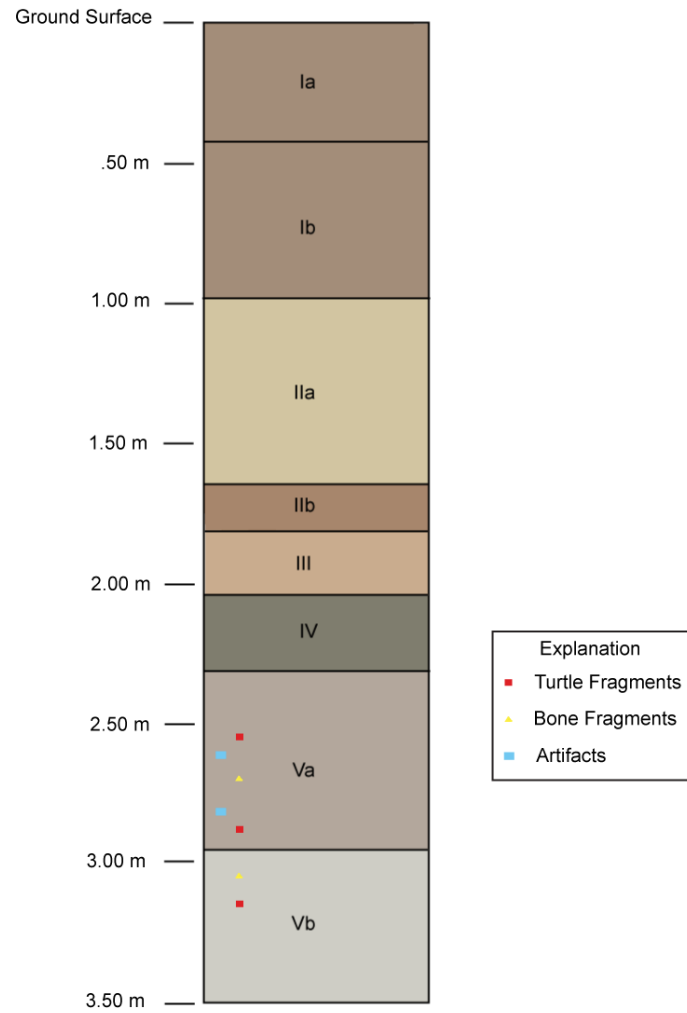


Figure 4. Adapted 2010 test trench stratigraphic column drawn by Deter-Wolf et al. 2011. The representative proveniences of both the faunal and lithic remains are recorded within the column.

2.2 Radiocarbon (^{14}C) Dates from Past Excavations

Radiocarbon dates from the 1994 excavation provided an age range between $27,050 \pm 200$ ^{14}C yr B.P. to $6,530 \pm 70$ ^{14}C yr B.P (Table 1) (Breitburg et al. 1996). The earlier date was taken from soil samples below the bone bed; the latter date was taken from organic soil within the bone bed (Breitburg et al. 1996). Only one charcoal sample was dated from the 1994-1995 excavation and dated to $31,594 \pm 220$ ^{14}C yr B.P. and was collected from below the mastodon bone bed (Table 1).

The majority of dates collected from the 2010 test trench were taken from organic sediment. One charcoal specimen was dated from what was believed to be bone bed horizon and dated to $12,050 \pm 60$ ^{14}C yr B.P. (Deter-Wolf et al. 2011); implicating that the deposits are pre-Clovis.

Table 1. Adapted table of radiocarbon dates from the 1994-1995 and 2010 excavations (Breitburg et al. 1996; Deter-Wolf et. al. 2011).

Radiocarbon Date ^{14}C yr BP	Lab Number/ Provenience	Date Recovered	Material
10,260 \pm 240	Above Bone Bed Beta-125351	1994-1995	Organic sediment
	Within Bone Bed		
12,030 \pm 40	Beta-125350	1994-1995	Organic sediment
12,050 \pm 60	Beta-288801	2010	Charcoal
	Under Bone Bed		
14,750 \pm 220	Beta-125352	1994-1995	Organic sediment
23,250 \pm 110	Beta-290991	2010	Organic sediment
26,810 \pm 200	Beta-80169	1994-1995	Charcoal
28,870 \pm 150	Beta-288802	2010	Charcoal

CHAPTER III

PHYSIOGRAPHIC SETTING

3.1 Topography

The site rests along the convergence of the Nashville Basin and the eastern edge of the Western Highland Rim. Regional topography is controlled by the uplift of the Nashville Dome, which was formed as the by-product of isostatic adjustment to erosion and is not seismically active (Huckemeyer 1999; Reesman and Stearns 1989). The uplift rates of the Nashville Basin for the past 100 million years are estimated to be 4.6 m per millennia (Reesman and Stearns 1989). The average elevation of the Highland Rim is over 300 m, whereas the Nashville Basin averages roughly 200 m in elevation, creating a giant crater-like structure.

The Coats-Hines site is 230 m above mean sea level, resting along the foothills of conical-shaped knobs, including Slider's Knob, less than 500 m to the east of the site (Figures 5 and 6). The summit of Slider's Knob is 344.12 m above sea level and is the highest peak of the surrounding hillslopes. Coats-Hines is bounded to the north by an intermittent, first-order stream that collects the erosional sediment and surface runoff from the eastern slopes and flows west, draining into Spencer Creek (Breitburg et al. 1996). Spencer Creek, in turn, continues to flow west, eventually draining into the Harpeth River, roughly 250 m north of Franklin, TN (Breitburg et al. 1996; Wilson and Miller 1963).

Coats-Hines Site (40WM31) Area Topographic Map

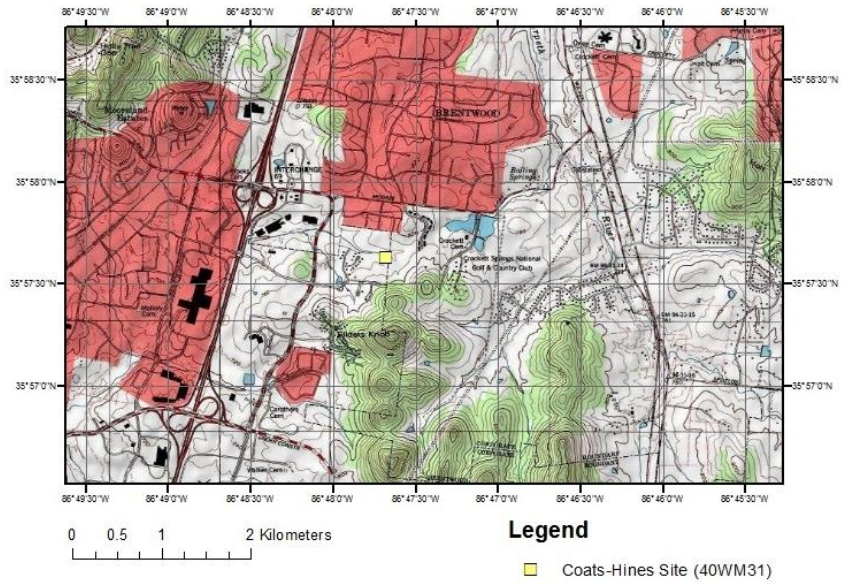


Figure 5. Topographic map of the Coats-Hines site.

Coats-Hines Site (40WM31) Area Topographic Map

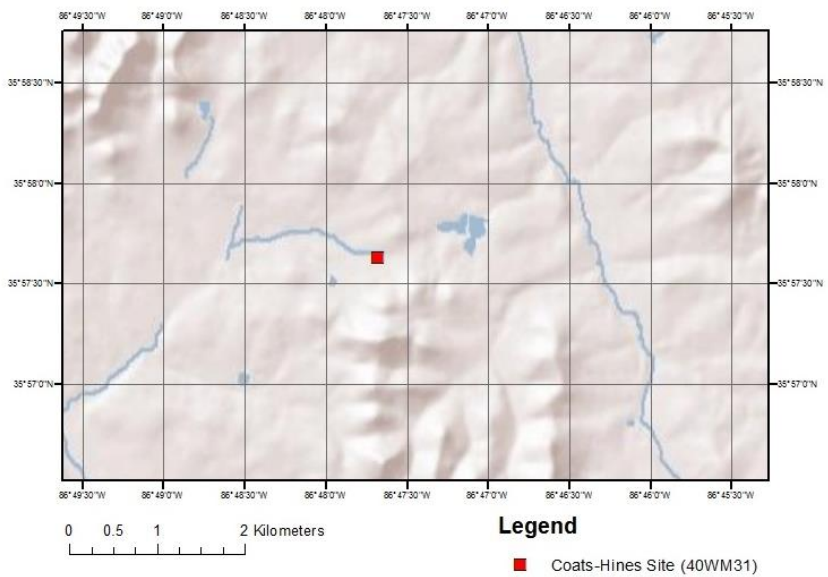


Figure 6. Topographic relief of the Coats-Hines site area.

3.2 Bedrock

The Nashville Basin is composed primarily of Ordovician limestone formations. The Highland Rim bedrock is mainly composed of Mississippian limestone interbedded with discontinuous Mississippian shale and sandstone lenses (Huckemeyer 1999; Wilson and Miller 1963). The site rests on the Ordovician Bigby-Cannon Limestone Formation which consists of three facies, the Cannon limestone, Dove-colored limestone and Bigby limestone which replace each other laterally and vertically (Wilson and Miller 1963). Bigby-Cannon limestone is composed of medium to coarse-grained limestone interbedded with microcrystalline and cryptocrystalline silicate nodules that have observed conchoidal fracture breaks (Wilson and Miller 1963). The knob formations to the east of the site are composed of the Ordovician Leipers and Cathes Formations as well as the Mississippian Fort Payne Formation and Chattanooga Shale. The Leipers and Cathes Formation are composed of fine-grained, fossiliferous, argillaceous limestone that precipitates phosphatic clay in residuum (Wilson and Miller 1963). The Fort Payne Formation consists of an upper cherty facies that vertically grades into thinly-bedded carbonaceous, laminated shale and minor amounts of medium-grained sandstone (Chattanooga Shale) (Wilson and Miller 1963)

Chemical weathering of the carbonate bedrock yields a highly dissolved load and thick deposits of clay throughout the region (Huckemeyer 1999). Phosphorous is found in the form of pellets within the Ordovician formation exposures in high enough amounts to be mined in the area. In addition, fluoride, lead, zinc, and barium are present within fissure veins of the Ordovician formations (Huckemeyer 1999). Chert is found in

the form of nodules (rarely bedded) within the Fort Payne and Bigby-Cannon Formations (Huckemeyer 1999). Elemental manganese and iron are present within the Mississippian formations; manganese is found in the form of low-grade psilomantane and iron in the form of limonite and goethite concentrations (Huckemeyer 1999).

3.3 Modern Climate

The modern climate of the region is described as humid continental, with warm, humid summers, and mild winters (Brakenridge 1984; Huckemeyer 1999). Hard freezes and snowfall are infrequent, and precipitation during the winter and fall seasons is generally from frontal systems. The yearly precipitation in the region averages 130 cm, with the majority of the precipitation occurring between late fall and early spring (Delcourt 1979; Huckemeyer 1999). The mean annual temperature for the Nashville region is 4.5° C in January and 27° C in July (Brakenridge 1984).

CHAPTER IV

GEOLOGY

4.1 Introduction

The goal of this analysis is to describe the alluvial/colluvial stratigraphy and depositional history of the occurring within the 2012 excavation pit and along the first order drainage bordering the site (Figures 1 and 3). The stratigraphy and soils as well as their properties including coarse sediment load and sorting, dates, and micromorphology are used to determine the landscape evolution, paleoclimate and rates of soil formation in the area (Huckemeyer 1999). In addition the laboratory analysis of the stratigraphic units revealed how the physical and chemical properties of the stratigraphic profile have changed over time. The site stratigraphy and depositional history of the Coats-Hines site are addressed in this chapter for a better insight into the context of the faunal and archaeological remains occurring at the site (Guccione 2008).

The unit classifications of Units 1 through 9, are based on both field and laboratory examination. Units 6a-c were not located within the 2012 excavation area, and therefore will be described in a separate section. Laboratory particle size analysis of the sediments was performed using the pipette method of analysis to definitively determine texture of each stratigraphic unit. Distribution of the particles size (mm) for unit samples collected from the east excavation wall is represented in Appendix B and C. The textural classification of the units was designated based on the percentages of sand, silt, and clay within the USDA textural triangle (Schaetzl and Anderson 2005). The particle size fractions for each unit are provided in the pipette analysis in Appendix B.

For the pipette analysis, roughly 200 g of sediment/soil was collected at 10 cm intervals from the modern surface through the base of the 2012 excavation floor from the East Wall of the Excavation (Figure 7) (Kilmer and Alexander 1949). Description of the coarse fragments in the unit descriptions is based on the field examination of the units and additional examination of the coarse fragments will be discussed in the separate gravel analysis section. The color classification is based on the Munsell soil color chart is described in the tables below using the dry consistence of the soil/sediment; further explanation of both the dry and wet consistence as well as the color classifications is located in Appendix B and Appendix C. In addition, the stratigraphic profiles of the excavation area are illustrated in figures 7,8, and 9.

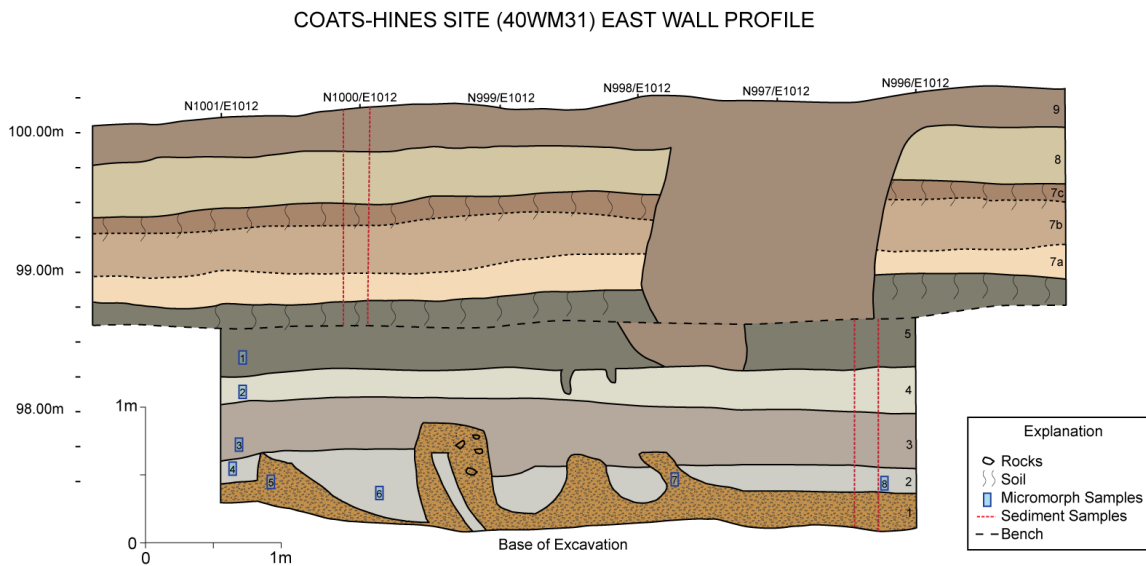


Figure 7. Coats-Hines site 2012 excavation, east profile wall.

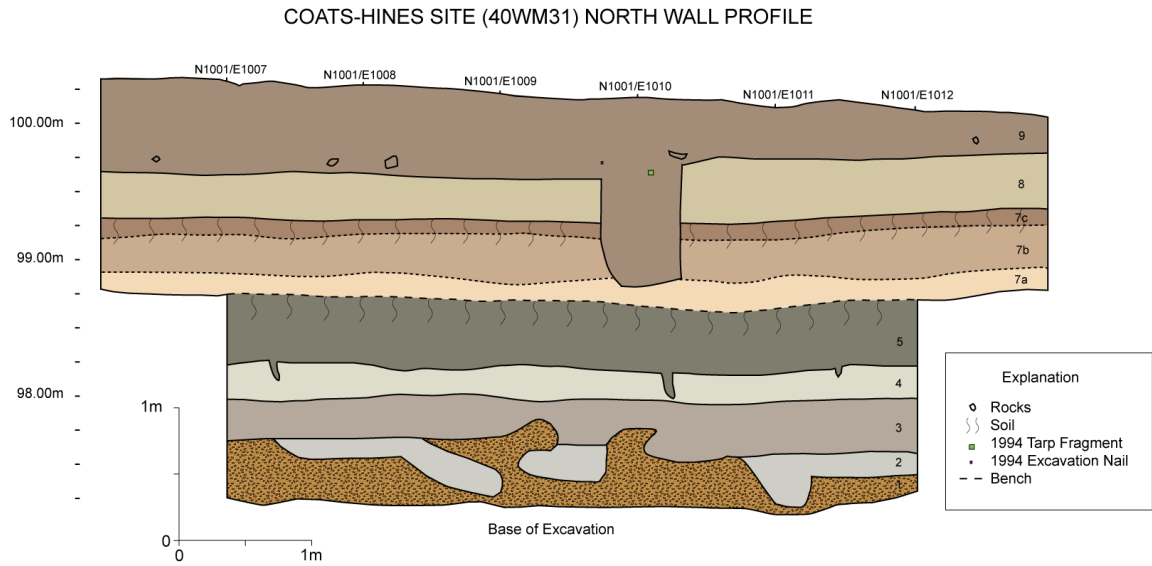


Figure 8. Coats-Hines site 2012 excavation, north profile wall.

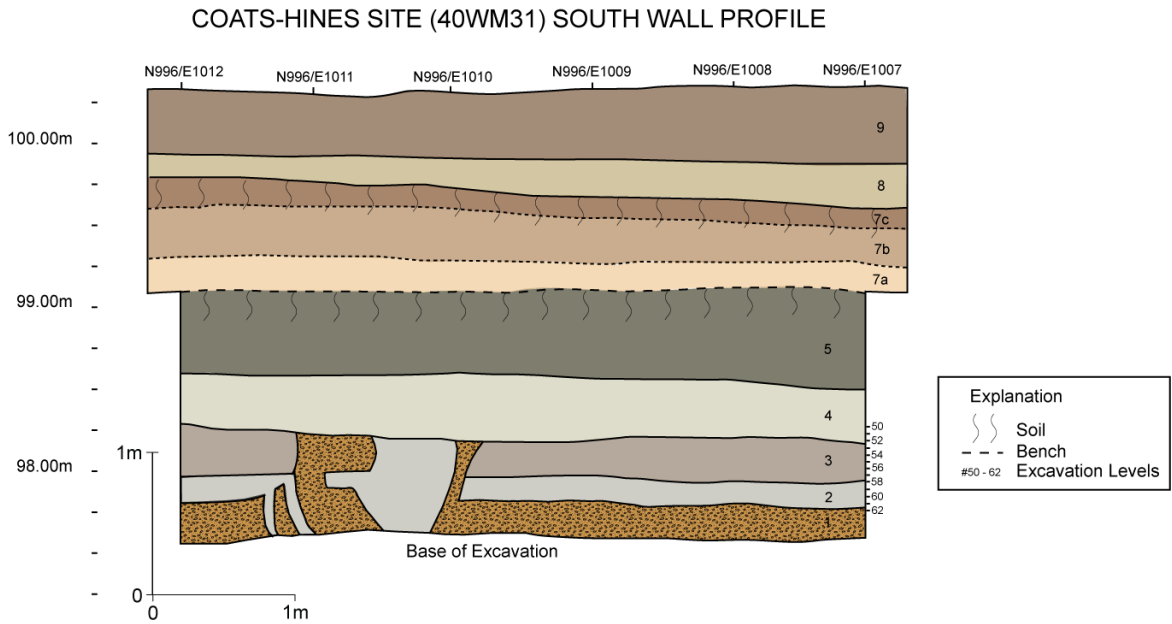


Figure 9. Coats-Hines site 2012 excavation, south profile wall.

4.2 2012 Excavation Area

The unit descriptions of the 2012 excavation are listed below and described from the ground surface to the base of the excavation. The depth was recorded from the ground surface.

Unit 9: (0-22 cm) is an anthropogenic, backfill package that consists of a brown (10YR4/2), very friable silt loam with a fine, structureless-massive structure. This unit is highly disturbed and discontinuous. Gravels in this unit range from 7 up to 15% in volume depending on the location in the excavation area, with the majority measuring between 2 to 5 cm in diameter, and the largest measuring 20+ cm. The majority of the coarse fragments in this unit are composed of angular, poorly sorted, limestone fragments. Presence redoximorphic features are little to none. Fine to medium-sized roots present at 7 to 10% by volume. Unit 9 terminates with a clear, relatively smooth boundary.

Unit 8: (22-55 cm) is a brown (10YR 4/3), friable, silty clay loam with structureless-massive structure; moderately sorted, limestone gravels are present between 2 and 3% by volume, measuring 2mm to 2 cm in diameter; decrease in abundance of fine to medium sized roots (5-7 %). No redoximorphic features present. The contact between Unit 8 and 7c is clear, smooth, and likely erosional.

Unit 7c: Ab (55-70 cm) is a dark brown (10YR 3/3) buried A horizon consisting of friable, silty clay loam with moderate, fine granular structure; minimal gravels (1-2%) measuring between 2 mm and 40 mm in diameter; few fine roots present at 2 to 3% by volume; no redoximorphic features and a clear, smooth boundary.

Unit 7b: Btb (70-100 cm) is a brown (7.5YR 3/2), friable, silty clay loam with secondary accumulations of clay films; structure of this unit is moderate, fine subangular blocky; few, fine, faint redoximorphic features; small, oxidized manganese nodules at 2-5% and measuring between 2-3 mm in diameter; few, fine roots present; very fine to fine coarse fragment at 2-3% by volume; clear, smooth boundary.

Unit 7a: Btb2 (100-120 cm) is a brown (10YR 4/3), friable, silty clay loam with few faint secondary accumulations of clay films on moderate, medium subangular blocky peds; few, fine, faint mottles; very fine to fine coarse fragments at 2-3% of the bulk sample; few, very fine roots present at 1-2%; abrupt (likely erosional), smooth boundary.

Unit 5: 2Btb(120-160 cm) is a very dark grayish brown (10 YR 3/2) firm, silty clay with moderate, fine, subangular blocky structure and secondary accumulations of illuvial clay along cracks and on ped surfaces. In addition, there are common, medium, distinct dark, yellowish brown (10YR 4/6) redoximorphic features and accumulations of iron and manganese nodules; increase in size and amount of coarse fragments (2-5%) and ranging between 2 mm to 16 cm in diameter, with an average diameter of 8 mm; few, very fine roots; abrupt (erosional) smooth boundary.

Unit 4: 2Btgb1 (160-180 cm) is a dark grayish brown (10YR 4/2) firm, silty clay with moderate, medium, subangular blocky structure and secondary accumulations of illuvial clay along cracks and ped surfaces; this unit is reduced with common,

fine, distinct nodules of manganese dioxide; limestone and chert coarse fragments at 3-5%, ranging in diameter from 2 to 16 mm, with an average of 8 mm; few very fine roots; presence of turtle (*Chrysemys* sp.) carapace and plastron fragments; abrupt, smooth boundary.

Unit 3: 2Btgb2 (180-210 cm) is a brown (7.5YR 4/2) firm, silty clay with moderate, medium, subangular blocky structure and secondary accumulations of illuvial clay films along cracks and ped surfaces; common, medium, prominent, strong brown redoximorphic features (7.5YR 4/6) in addition to manganese and iron concretions; increase in coarse fragments at 5-7% by volume and ranging from 2 to 32 mm with an average of 8mm; very few, very fine roots; small bone scatters dispersed throughout the unit at 2-3% abundance, increasing with depth; small rodent burrows averaging 5 cm in diameter present at the top of the unit, little to no burrows noted towards the base; abrupt, irregular boundary.

Unit 2: 2Btgb3 (210-235 cm) is a gray (10YR 5/1) firm, clay with moderate, medium, subangular blocky structure and secondary accumulations of illuvial clay along cracks and ped surfaces; few, fine to medium, distinct strong brown redoximorphic features (7.5YR 4/6) as well as small manganese and iron concretions (plinthite and goethite); increase in abundance and size of limestone and chert coarse fragments, with 7-9% by volume and measuring between 2 and 64+mm in diameter, with an average of 8mm; very few, very fine roots; bone scatters at (2-5%) including mastodon tooth fragments, turtle shell, and Pleistocene megafauna bone fragments; abrupt, irregular boundary.

Unit 1: 2Btb (235-260 cm) is a strong brown (7.5YR4/6) firm, gravelly clay with moderate, medium, subangular blocky structure and secondary accumulations of illuvial clay; common, medium, prominent grayish brown (10YR 5/2) reduced features present with frequent accumulations of manganese and iron concretions; increase in gravel size and abundance, with 10-15% abundance and a range of 2 to 64 mm with an average between 8 and 16 mm in diameter; increase in bone fragments and size, bones are heavily replaced with iron; no roots present; abrupt, irregular boundary.

4.3 Macromorphology: Turbation Features

The bottom three units of the excavation area contain abrupt, irregular contacts in confined areas that are discontinuous throughout the site. The features are bowl-shaped with infill of reduced clay and adjacent mounds of gravelly, oxidized clay (Figure 10). Pit and mound microrelief is often interpreted as a cryogenic feature, or cryoturbation (Embleton-Hamann 2004). Since the Coats-Hines site is beyond glacial and periglacial conditions, and was therefore never cold enough to develop cryoturbation features, this study proposes an alternative hypothesis. An additional hypothesis is that the soft sediment deformation features were created as a result of paleoseismic activity, convoluting the lower three units. Given that no significant seismic events have been recorded in the site area, this hypothesis was dismissed. The cradle-and-knoll topography seen in the lower levels of the excavation are also typical features created by treethrow, or arboturbation in which sediments and soils can be buried, mixed, or brought to the surface (Waters 1992).

Treethrow, or “arboturbation” is formed when a tree falls over, creating a crater where the roots once were and adjacent mounds where soil and gravel slumps off the roots (Schaetzl and Anderson 2005). Treefall contorts, mixes, and overturns soil horizons in a profile, having the potential to double the thickness of a single unit (Schaetzl and Anderson 2005). Treethrow stratigraphy can appear somewhat convoluted from the displacement and contortion of lithologic units. The treethrow pit is a zone of stronger leaching, the pore space created by the decayed roots of the tree allow water to move through the profile. Distinguishing treethrow features is also important for the study of paleoenvironment in that it occurs most commonly, in forested areas.

When the roots of the fallen tree decay, infilling from upper horizons can penetrate into the units below, such as what occurs in the excavation area where Unit 2 has infilled into the treethrow pits (Figure 10). The low permeability of the Unit 2 soils maintains the reduced conditions and color of Unit 2 within the tree pit. In addition coarse clasts from Unit 1 were displaced into Unit 2 and 3 by uprooting, creating concentrations of gravel in the uprooting mounds, as seen in Figure 7, 8, 9, and 10 (Schaetzl and Anderson 2005). Gravels with a diameter of 64+ mm are not observed in Unit 3, except within the uprooting mounds, in which gravels were uprooted from Unit 1. Planview of the excavation area in the bottom three units, show channel-like, oxidized sediment with gravelly clay infill which was formed from the collapse of decayed roots that were filled with the surrounding sediment, creating soft sediment root casts (Waters 1992).

The uprooted soil of Unit 1, 2, and 3 were later covered with the silty clay of Unit 4, leveling the cradle-and-knoll topography. If the treethrow features were exposed to the surface they would be subject to weathering and erosional processes. Since the cradle-and knoll topography was preserved in the substrate it is unlikely that the deformation was exposed at the surface for a long period before being covered by the silty clay of Unit 4. In addition, it is likely that the cohesiveness of the soil in the lower units helped maintain the structure of the turbation features.



Figure 10. Treethrow features along the east wall of the 2012 excavation pit.

4.4 Micromorphological Analysis

4.4.1 Introduction to Micromorphology

Micromorphological analysis is useful for the interpretation of various aspects of archaeology and geology. Examination of the various components and arrangement of the sediment and soil matrix of a thin section is used to determine if the sample has a pedogenic fabric (Schaetzl and Anderson 2005; Stoops 2003). In addition, micromorphological analysis is useful in determining whether or not certain depositional and post depositional processes have influenced the stratigraphic record of the site (Rapp and Hill 2006). The mineral and clast analysis within micromorphological thin sections can be used to determine sediment sourcing, and the given shape, size, and orientation of the particles and matrix one can potentially determine the geomorphic nature of deposition. Certain structures within a thin section are the result of climatic processes/changes and therefore can be used for the interpretation of the paleoclimate of a region (Fitzpatrick 1984; 1993). Finally, the context, and therefore the age, of radiocarbon samples in a profile can be validated through micromorphological analysis, which is important for reporting early archaeological sites.

4.4.2 Methods of Micromorphological Analysis

Eight micromorphological samples were retrieved to be thin sectioned, from the bottom five units of the East Wall (Figure 7; Table 2). The samples were collected in the lower five units because these were the geological units that were bone-bearing and based on correlation with previous excavations, potentially contained archaeological remains. In addition, the bottom three units (Units 1, 2, and 3) contained irregular stratigraphy in

some areas of the excavation, including along the East Wall that had yet to be conclusively defined. Samples 1 through 4 were collected along the northern edge of the East Wall, where there was relatively normal stratigraphy. Samples 5 and 7 were collected from Unit 1 in the areas of irregular bedding. Finally, samples 6 and 8 were both collected from Unit 2 to determine the relatedness of the sediment within this unit. The goal of the micromorphological analysis was to determine the relatedness between units, determine the lithology/mineralogy of each unit to discern the provenience, or ultimate source of the clastic sediments, the soil/plant/root relationships, and the microstructure of the peds and turbation features.

The samples were collected in frames that measured (length × width × height) 5 cm × 5 cm × 5.5 cm, collecting approximately 131.1 cubic centimeters of sediment. The samples were impregnated with epoxy resin, hardened, and commercially thin-sectioned for micromorphological analysis (Fitzpatrick 1984; Driese et al. 2005). The thin sections were examined using both plain polarized and cross polarized light through a polarizing petrographic microscope and observed at low (1.25× and 4×), medium (10×), and high objectives (40×) (Klein and Dutrow 2008; Stoops 2003).

Table 2. Stratigraphic unit and micromorphological sample correlation.

Micromorphological Thin Sections: Unit Correlations	
Geologic Unit	Sample #
5	1
4	2
3	3
2	4, 6,8
1	5, 7

4.4.3 Interpretation of Micromorphological Thin Sections

From the micromorphological analysis of the thin sections, it was determined that all five units were argillic B horizons with weathered subangular blocky structure secondary accumulation of illuvial clays as seen in the longitudinal and cross sections of root pores and ped surfaces (Figures 11-16). The clay bands have continuous orientation and therefore were originally deposited in that way (Fitzpatrick 1984). The accumulation of clay coats along root pores and between peds occasionally forms plugs in the pores of the soil matrix of the lower units. Larger particles and concretions allow the alignment of clay particles parallel to their margins, often forming concentric bands (Fitzpatrick 1984; 1993). Accumulation of these bands on sand and gravel as well around peds (cutens) formed bridge structures in areas of the thin sections.

Unit 5 was thought to be a buried A horizon because of its low color value, therefore it was suspected to contain a high amount of organic matter. Upon examination of the thin section sample, what was thought to be organic matter was in fact a high amount of manganese dioxide staining and concretions (Figure 11). In addition, ferric hydroxide and goethite concretions occur very frequently, also contributing to the paleosols color. The areas of Figure 12 that are predominately brownish-yellow and/or reddish-yellow, the principal coloring substance is iron, or iron oxide (Fitzpatrick 1984; 1993). Goethite-coloring indicates a “hydrated” matrix (Fitzpatrick 1984). Figure 12 is a plain polarized projection of a root pore with banded illuvial clay coats; which is typical in all five units. The laminated fabric of Figure 11 and 12, expressed by bands of clay

also support the conclusion that this soils was periodically saturated/hydrated (Brewer and Sleeman 1988).

Unit 4 is unique in that it is extremely reduced, with rare staining of iron- or manganese-oxides, although goethite and manganese concretions do occur in this unit in the form of spherical and semi-spherical glaebules (Figure 13). The dominant depletion pedofeatures are the result of a saturated environment (Schaetzl and Anderson 2005). The concretions of manganese dioxide with compound coatings of illuvial clay and ferric hydroxide, occasionally include silt and sand grains within the concentric coatings (Fitzpatrick 1984). Compound coatings also occurred along root pores within this unit (Figure 13). In addition, as seen in Figure 14, small ovoid and granular faecal pellets, likely from enchytraeid worms to earthworms, were found in clusters within vermiforms occasionally in the soil matrix of all five units. The incorporation of sand grains within the clusters of faecal material is typical of vigorous earthworm activity (Fitzpatrick 1993; Schaetzl and Anderson 2005).

Unit 3 contains more oxidation features compared to thin sections from Units 2 and 4. Accumulations of weathered fossiliferous limestone and chert clasts occurred throughout the lower profile, originating from the Mississippian bedrock upslope; although, fossilized crinoid stems were observed, most prevalently in Unit 3, with preserved cell structure.

Unit 2 appears very similar to Unit 4 in that it is extremely reduced, containing a gleyed matrix due to ferrous compounds that are found in soil horizons that are temporarily or permanently saturated with water (Fitzpatrick 1993). The saturated

environment of Units 2 and 4 are likely the result of a perched water table. Precipitation periodically flowed through the profile gravitationally depositing illuvial clay in lower horizons and as a result increased the bulk density and reduced the permeability of the lower units (Driese et al. 2005). Redoximorphic features are abundant through the lower profile, but concentrated in Units 2 and 4, where the water table became perched due to the low infiltration rates of the clay peds within these units. In addition, charcoal roughly retaining its original cellular structure was discovered in Sample 4 of this Unit (Figure 15).

Unit 1, in contrast to Unit 2, is abundantly oxidized, containing very frequent accumulations of goethite concretions (Figure 16). In addition there is an increased frequency of sand and gravel-sized rock in random distributions.

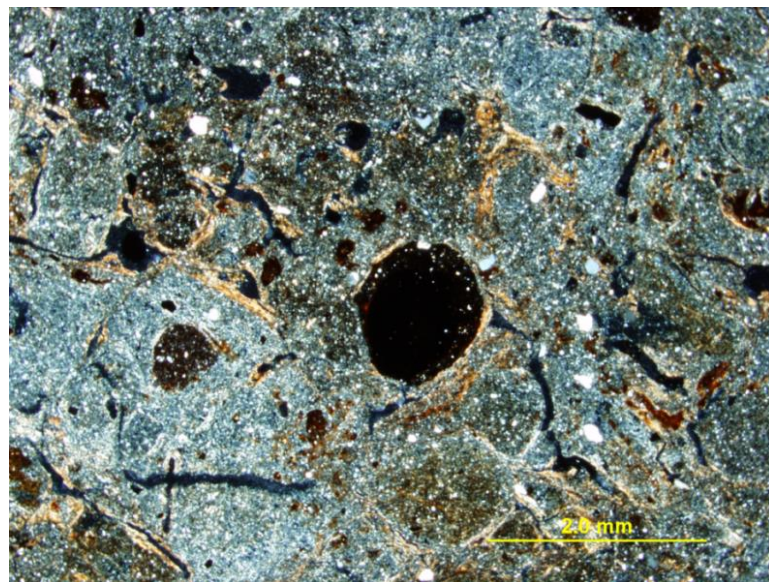


Figure 11. Manganese concretion, lateral illuvial clay coats in root pores, Unit 5, Sample 1, XPL, 1.25× magnification.

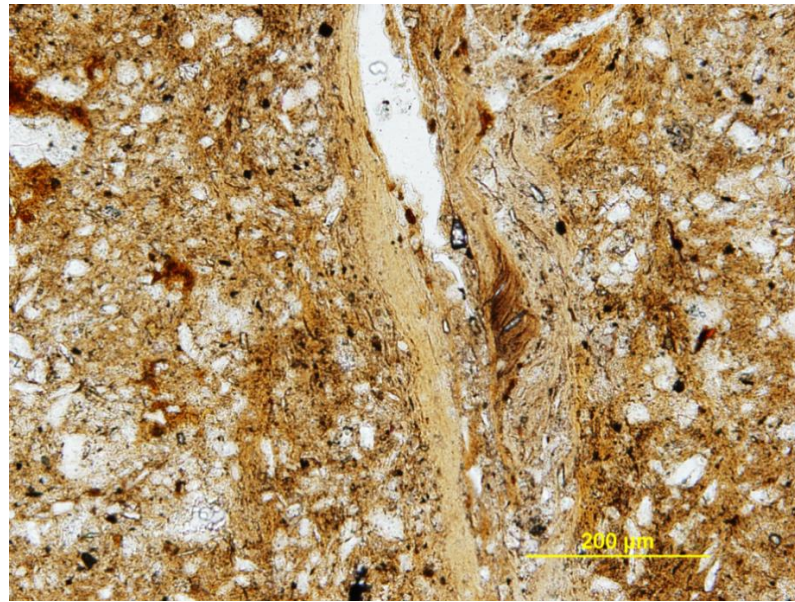


Figure 12. Banded illuvial clay, Unit 5, Sample 1, PPL, 10 × magnification.

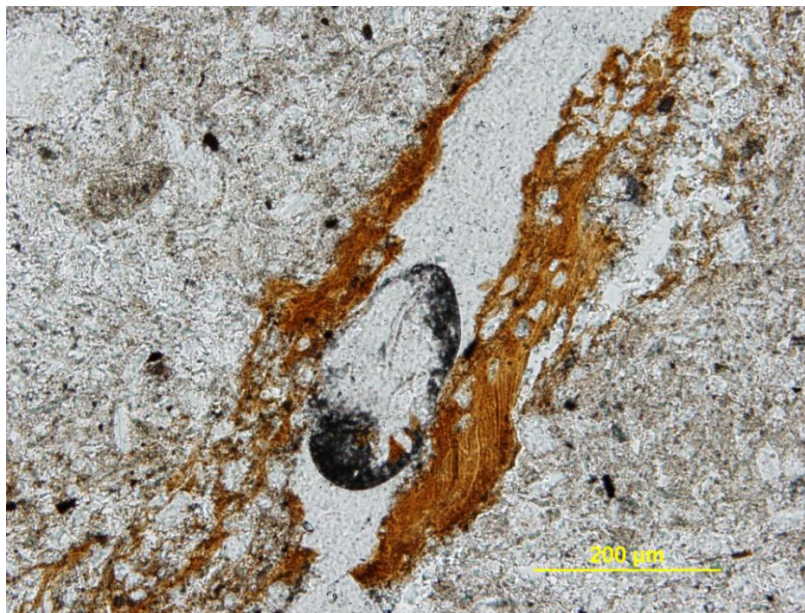


Figure 13. Banded clay in root pore, depleted matrix, Unit 4, Sample 2, PPL, 10× magnification.

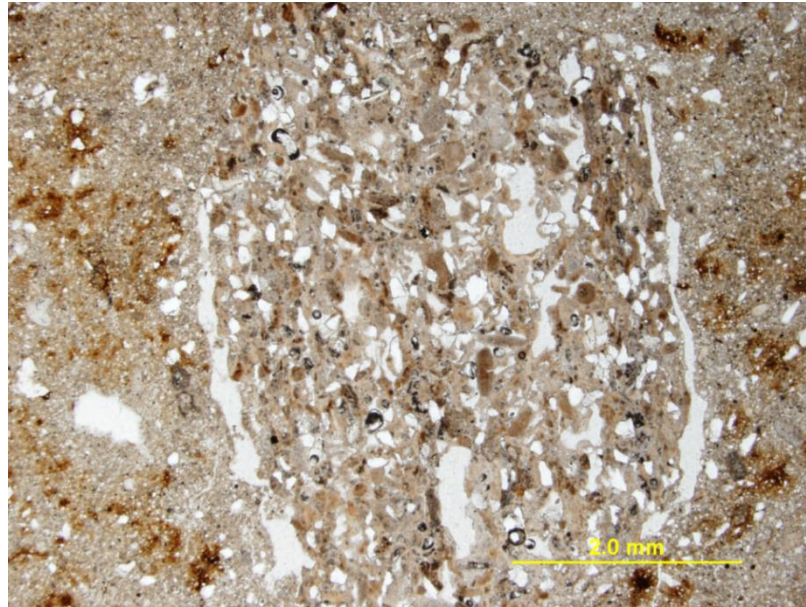


Figure 14. Faecal pellets, Unit 4, Sample 2, PPL, 1.25 × magnification.

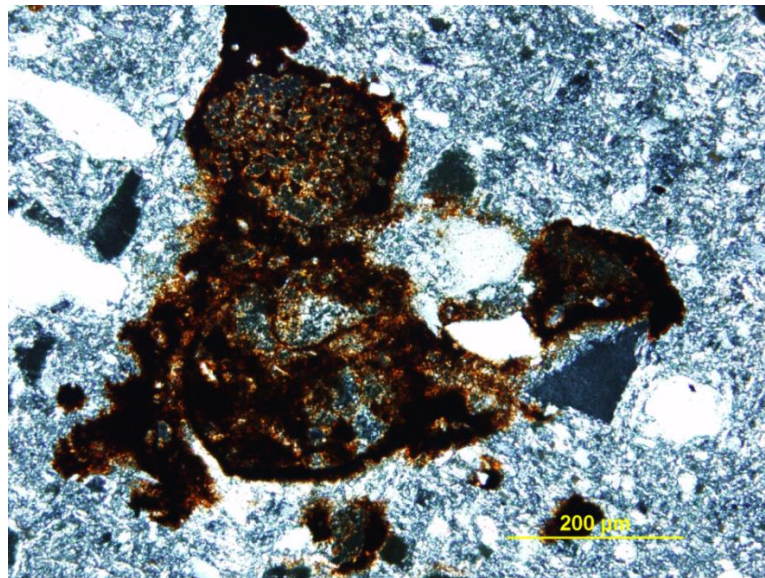


Figure 15. Charcoal with cellular structure, Unit 2, Sample 4, XPL, 10× magnification.

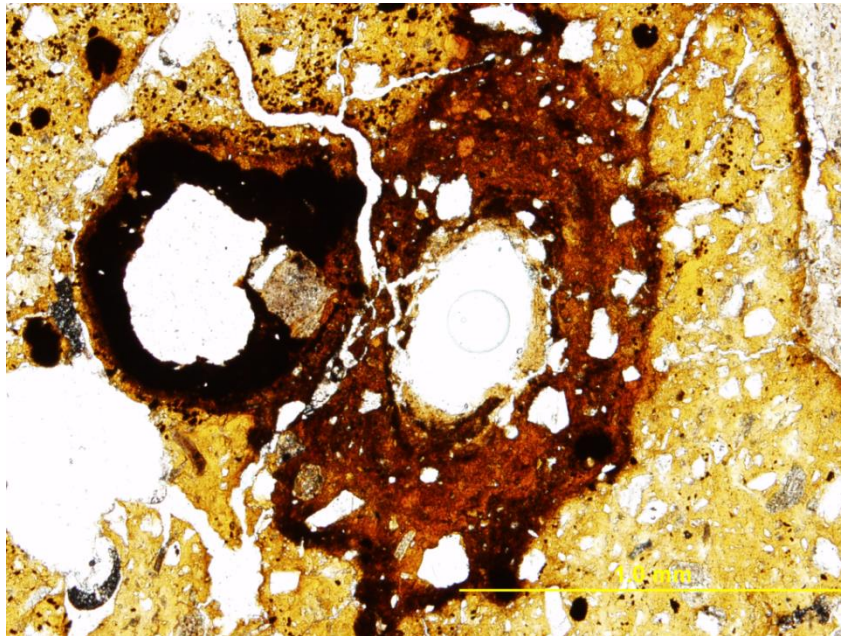


Figure 16. Iron Concretion with composite coating, Unit 1, Sample 7, PPL 4× magnification.

4.5 Gravel Distribution

4.5.1 Introduction to Coarse Fragments

Clastic materials (mineral and rock fragments) comprise a soil/sediments skeleton (Schaeztl and Anderson 2005). The roundness, sphericity, and composition of a particle can provide useful information in the distance it traveled from its original source. Although roundness and sphericity are typically used for the analysis of sand-sized clasts, they were applied to this study to determine the extent of weathering processes. Roundness is the smoothness/roughness of a particle; increased roundness indicates increased erosion and likely greater distance traveled. Sphericity is the measure of how flat/spherical the particle is increased sphericity also can indicate increased erosion and distance traveled. The roundness and sphericity are not only dependent on

erosion and the original size of the grain surface, but the hardness of the clast which is dependent on the clast composition; softer rocks/rock fragments will erode faster than harder rocks/rock fragments (Rapp and Hill 2006).

Sphericity related to the overall shape of a clast, and is measured by the degree to which the gravel resembles a sphere. Roundness is the measure of how much a particle's corners and edges are smoothed and is a function of the velocity the gravel is transported and the process/roughness of transportation and deposition (Whitehouse 2004). Coarse clasts often become more rounded and spherical as they get more weathered (Schaeztl and Anderson 2005). Poorly sorted, large, rough gravels, with) indicate high energy flow with rapid deposition. In addition, coarse fragments affect the manner in which water moves through and is retained in the soil/sediment profile. Water will move rapidly through coarse-textured soils because the gravel fragments have larger pores and minimal surface area to attract water within the soil matrix (Schaeztl and Anderson 2005).

The goal of the gravel analysis is to determine the source of the gravel clasts, the nature in which they were deposited, and the relatedness of the gravels between Units based on composition and similar size and extent of weathering.

4.5.2 Methods of Gravel Analysis

A representative sample from Unit N996/E1008 was used to estimate the gravel distribution at the site. It would be too difficult to obtain the data on coarse fragment content for the entire site, and given the treefall features, as seen in Figure 10, the data could be skewed from post-depositional processes redistributing gravel clasts. Unit

N996/E1008 is positioned along the south wall of the 2012 pit (Figure 9) and was selected because it is in an area of the excavation pit with normal, unturbated stratigraphy. The gravels were collected and analyzed based on the arbitrary units in which they were excavated and therefore only represent the lower four lithologic units (Unit 1, 2, 3, and 4) (Figure 9). The arbitrary levels were excavated in 5 cm increments, beginning at level 51 (97.950-97.900 m) and ending at level 61 (97.450-97.400) (Figure 9).

The gravels from Unit N996/E1008 were collected with the bulk sample by excavation level; and later screened, washed, and size-sorted using a dry-sieve method (Figure 9). The sieves sorted the gravels into different size classes based on the clast diameters described by the Wentworth Grain-Size Classifications (Figure 17). The Wentworth Grain-Size Classification organizes gravels into granules (2 mm), small pebbles (4 mm), medium pebbles (8 mm), large pebbles (16 mm), very large pebbles (32 mm), and cobbles (64 mm and greater). The bulk weight as well as the weight of each size class within a level was recorded. In addition, each level was sorted and weighed by composition (i.e. mineral or rock type). To test the roundness and sphericity of the gravel clasts, the gravel in each level was sorted based on the roundness and sphericity chart, adapted from Krumbein and Sloss (1963) (Figure 17). The roundness and sphericity chart is used as a guide to determine the extent of weathering a clast has undergone; the higher the number, the greater the amount of weathering (Krumbein and Sloss 1963).

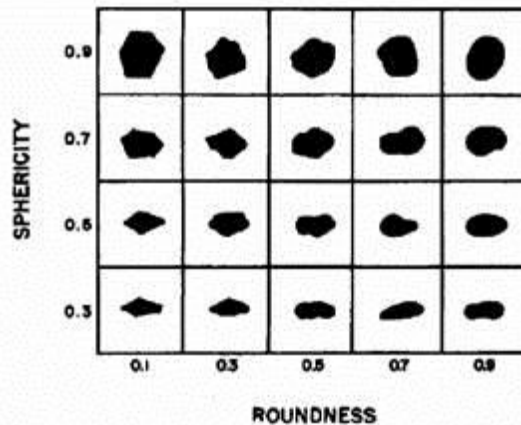


Figure 17. Roundness and sphericity chart (Krumbein and Sloss 1963)

Roundness of the gravels from each level was determined for all gravels larger than 2 mm. The sphericity of the gravels from each level was determined for all gravels larger than 4 mm. The interpretation of the roundness of the gravels was based on the average volume for each roundness classification in a level. The interpretation of the sphericity was based on the 8 mm size class (medium pebble) due to the larger size classes were not well represented in every level. For further description or data collected from the gravel analysis, see Appendix E.

4.5.3 Results of Gravel Analysis

4.5.3.1 Composition

The composition of the gravels analyzed from Unit N996/E1008 consists of limestone, chert, and sandstone (Figure 18). The majority of the composition (95.3%) is limestone, with minimal chert clasts (4.4%), and statistically insignificant portions of sandstone (0.3%). The limestone originated from the bedrock in the area, physically weathering, and being transported into the site area from upslope. Similarly, the chert

clasts are found in nodules precipitating out of the bedrock in the region, and likely weathered and was transported and deposited from the bedrock upslope. Limestone dominates the clast composition because it is the most abundant rock-type in the region as well as being a softer rock and more susceptible to chemical weathering, compared to chert, and is therefore easier to erode and redistribute.

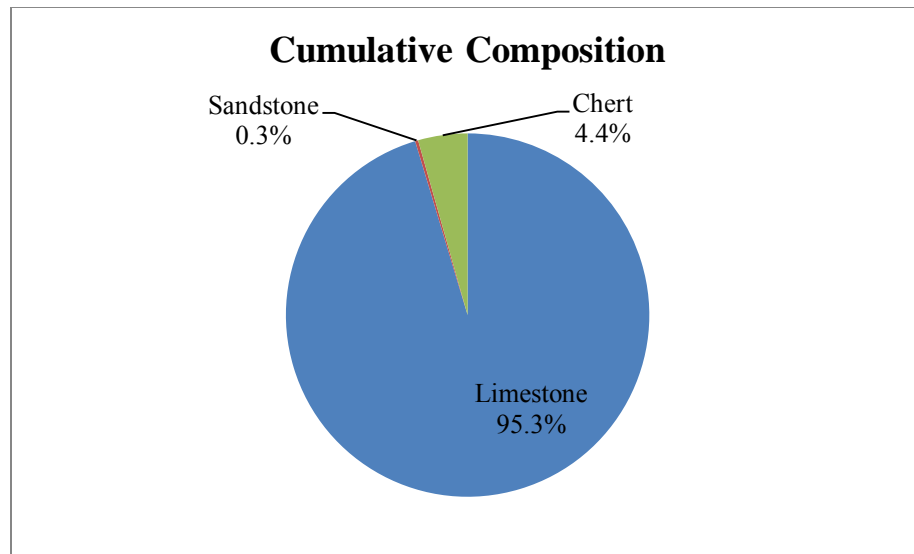


Figure 18. Cumulative (Levels 51-61) composition of the gravel clasts in excavation levels 51-61 (Units 1-4).

4.5.3.2 Weight Distribution of Gravels

The results of the gravel weight distribution is useful in confirming the Unit boundaries described in the previous discussion of the site stratigraphy based on the fine grained fraction (smaller than 2 mm). Figure 19 shows relatively low volumes of gravel for Level 51 and 52 (97.950-97.850 m). Level 51 and 52 are both within Unit 4 of the profile (Figure 19). Level 53 through 56 (97.850-97.700 m) have a moderate increase in gravel volume, indicating that they were deposited in a higher energy environment that

could weather and transport an increased load of coarse-grained deposits. Level 53 through 56, were therefore determined to be lithologically distinct from Level 51 and 52, and therefore grouped into Unit 3. There is a significant increase in gravel volume between Levels 57 and 60 (97.700-97.650 m), coinciding with Unit 2. Finally, the highest volume of gravel was from Level 61, which coincides with Unit 1 (Figure 9).

It should also be noted that there was an increase in the size of gravels with Levels 51 and 52 not containing gravels larger than 16mm and Levels 53 through 58 not containing gravels larger than 31.5 mm. In addition, the average size in diameter for all four units is 8 mm in diameter, as determined by total weight distribution by size in each level (Appendix E).

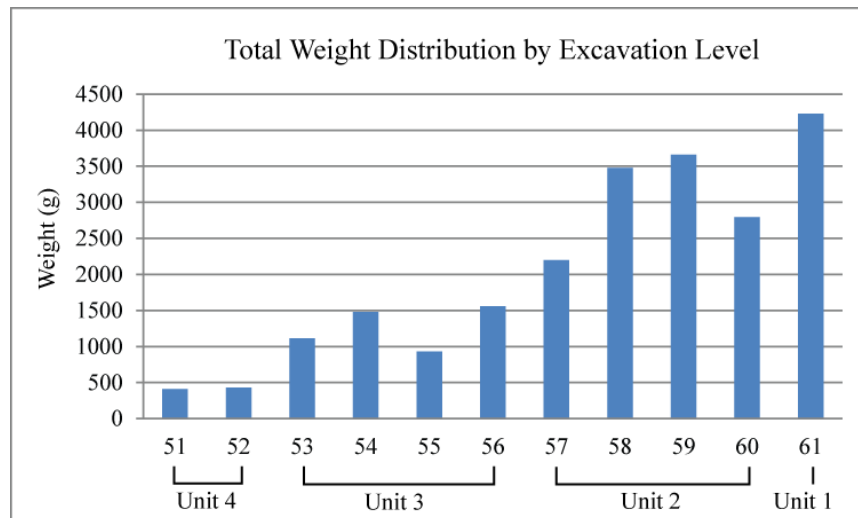


Figure 19. Total weight (g) of each excavation level of Unit N996/E1008 and their associated geologic unit.

4.5.3.3 Roundness and Sphericity

Roundness and sphericity are relatively constant throughout the lower profile, with the exception of the Unit 4 gravels (Level 51 and 52) and the Unit 1 gravels (Level 61). Generally, the gravels in Units 1 through 4 are subangular/subrounded (.5) with a spherical (.5) shape. This indicates that they were likely eroded from the same location, under similar depositional energy.

The roundness of the gravels in Unit 4 are equally distributed, between very angular and well rounded (.1-.9) (Figure 20), rather than the majority of the gravels being subangular/subrounded (.5). The sphericity of the gravels in Unit 4 are comparable to the results for the rest of the profile with the exception of Unit 4 containing higher rates of prismoidal (.3) clasts. The majority of the gravels in Unit 4, like Unit 3, 2, and 1 are spherical (.7). The discrepancy of the roundness values in Unit 4 (Level 51 and 52) could be the result of the small sample size/abundance of gravel in Level 51 and 52. In addition, the sizes of the gravels in Unit 4 are smaller in diameter, compared to the other three units. Smaller clasts have less surface area to weather and erode and therefore tend to be more angular, depending on the depositional environment. Based on the field and micromorphological analysis it is not likely that the gravels from this Unit, originated from a different source from that of Unit 1, 2, or 3.

Unit 1 (Level 61) has a significantly higher amount of gravels that are spherical (.7) but otherwise is comparable to the gravels of the other three units (Figure 21). The increase in spherical gravels could be due to the overall increase in the amount of gravel found in Unit 1. Spherical gravels are the most common in the profile, and Unit 1 simply has more creating a spike in abundance.

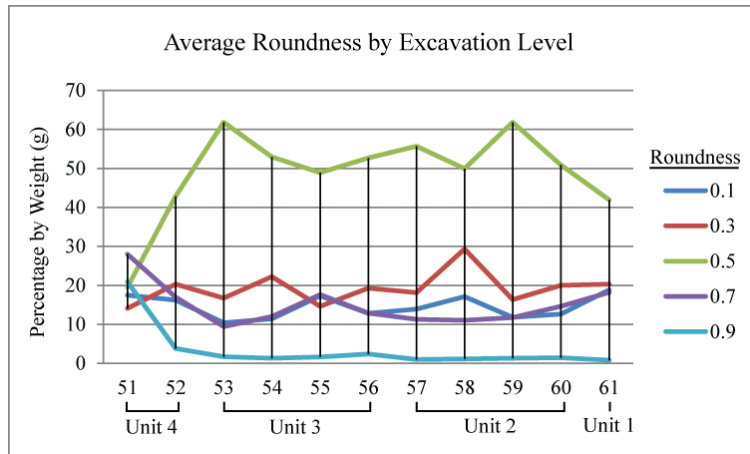


Figure 20. Roundness of gravels in excavation levels 51-61 of Unit N996/E1008. Presented using the average weight (%) of each roundness classification per level.

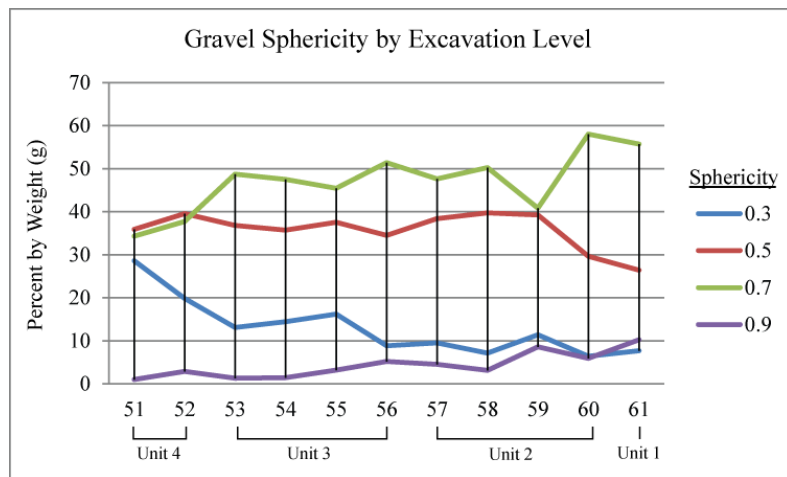


Figure 21. Sphericity of gravels in excavation levels 51-61 of Unit N996/E1008. Presented using the percentage by volume of each sphericity classification by level.

4.5.3.4 Interpretation

Given the composition, weight distribution and shape of the gravels found in the lower profile of the 2012 excavation area, it was determined that the gravels eroded from

the Mississippian limestone and chert bedrock from upslope. The gravels were transported equal distances and therefore had similar shapes throughout the profile. The gravels of Unit 1 were likely eroded from exposed bedrock upslope and deposited during a high energy, erosional event based on both the size and sorting of the gravels. The bedrock upslope became buried or less exposed to weathering, causing the decrease in size of gravels being transported into the site. By Unit 4, most of the gravels that would be weathered from upslope are deposited at the site. The Holocene paleosol capping Units 1-5 contain well-sorted fine grained sediment representing a shift to low-energy colluvial deposition of hillslope sediment.

4.6 Dates from the 2012 Excavation

A problem with previous excavations at the Coats-Hines site is the lack of radiocarbon dates taken on charcoal. Many of the previous dates were poorly provenienced and taken from bulk sediment samples, which provide a minimum age. As Breitburg and Broster (1995; 22) stated in their summary of the Coats-Hines site, “unless the find is carefully documented, ... enough scientific evidence cannot be claimed to prove the site’s authenticity.” Therefore, one of the goals for the 2012 excavation was to establish the archaeological context of the remains with solid radiocarbon dates.

The high humidity and temperate climate of the region tends to rapidly oxidize and decay organic material for dating. Fortunately, the relatively anaerobic conditions of the dense clay in the bottom four units of the excavation area aided in the preservation of charcoal specimens. Unit 7 and 8, by comparison, had little to no organic material,

including charcoal, to date and will thus be dated based on archaeological and terrace correlation from other regional studies (Huckemeyer 1999).

Table 3. 2012 radiocarbon dates.

<u>UCIAMS-</u>	<u>SAMPLE TYPE</u>	<u>LOCATION</u>	<u>CHEMICAL FRACTION DATED</u>	<u>Radiocarbon Age ¹⁴C yr BP</u>	-	-
UCIAMS-120329	CHARCOAL	Geologic Unit 4	ABA CHARCOAL	22,490	±	100
UCIAMS-120330	CHARCOAL	Geologic Unit 3	ABA CHARCOAL	26,290	±	150
UCIAMS-120331	CHARCOAL	Geologic Unit 3	ABA CHARCOAL	36,120	±	480
UCIAMS-121950	CHARCOAL	Geologic Unit 3	ABA-NITRIC ACID CHARCOAL	36,590	±	650
UCIAMS-120332	CHARCOAL	Geologic Unit 3/2	ABA CHARCOAL	31,140	±	270
UCIAMS-121951	CHARCOAL	Geologic Unit 3/2	ABA-NITRIC ACID CHARCOAL	30,910	±	320
UCIAMS-120333	CHARCOAL	Geologic Unit 2	ABA CHARCOAL	30,740	±	240
UCIAMS-120334	CHARCOAL	Geologic Unit 2	ABA CHARCOAL	26,310	±	150
UCIAMS-120335	CHARCOAL	Geologic Unit 1	ABA CHARCOAL	30,620	±	240
UCIAMS-120336	CHARCOAL	Geologic Unit 1	ABA CHARCOAL	>26,400	±	---

The radiocarbon dates from the 2012 excavation are listed in Table 3, further information on the dates is provided in Appendix F. In addition a core with the generalized stratigraphy of the 2012 excavation pit contains the radiocarbon dates with their associated elevations (Figure 22). The charcoal sample from Unit 4 dated to 22,490 ± 100 ¹⁴C yr BP (UCIAMS-120329), and was taken from Level 50 at an elevation of 97.961 m and is therefore near the bottom of the unit. Unit 3 dates between 26,290 ± 150 ¹⁴C yr BP (UCIAMS-120330) and 36,590 ± 480 ¹⁴C yr BP (UCIAMS-121950) (Table 3). The samples were taken from Level 52 at an elevation of 97.880 m near the top of the Unit and Level 55 at 97.744 m in elevation in the middle to bottom of Unit 3. The early date of 36,590 ± 480 ¹⁴C yr BP (UCIAMS-121950) is likely from charcoal uprooted into Unit 3 from lower units. Unit 2 dates between 26,310 ± 150 ¹⁴C yr BP (UCIAMS-

120334) and $30,740 \pm 240$ ^{14}C yr BP (UCIAMS-120333) , indicating relatively continuous deposition. The charcoal samples for Unit 2 were taken from Level 59 at elevations of 97.546 m and 97.520 m. Finally, Unit 1 dates to $30,620 \pm 240$ ^{14}C yr BP (UCIAMS-120335), and was collected in Level 62 at an elevation of 97.394 m.

COATS-HINES SITE (40WM31) 2012 RADIOCARBON DATES

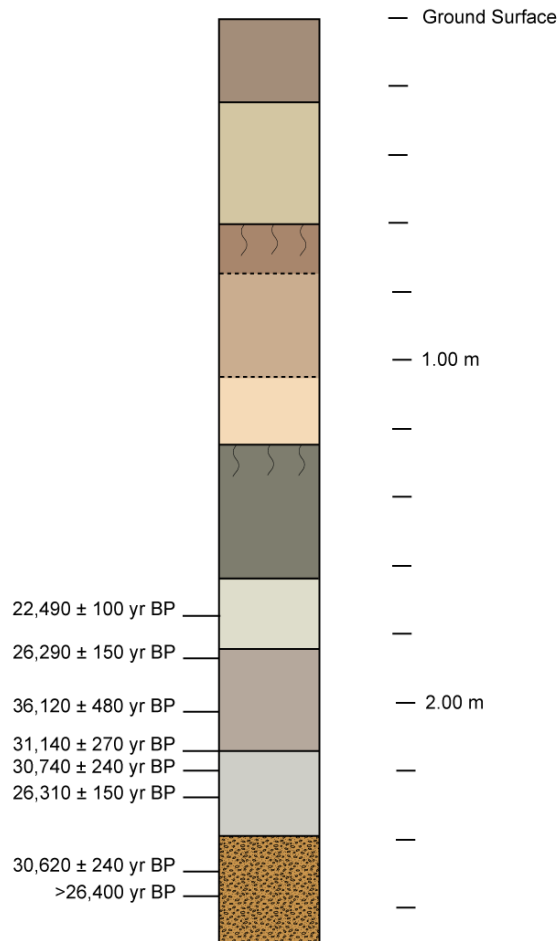


Figure 22. Generalized core of 2012 excavation units with associated radiocarbon dates (^{14}C yr BP).

4.7 Channel Unconformity

4.7.1 Introduction

In March of 2013 the wet-weather drainage was surveyed to determine when and how the remains of Mastodon B from the 1994/1995 excavation were deposited along the drainage. Evidence of a channel unconformity was discovered at Locality I and II along the banks of the drainage and area described below (Figures 1, 23, and 24). No charcoal was discovered during the investigation of the channel, and therefore the geochronology of the sediments in the following units will be based on regional correlations discussed in later chapters of this thesis.

4.7.2 Unit Descriptions

Unit 6c:Bw1 (120-185 cm) consists of a brown (7.5YR 5/4), firm, slightly gravelly clay with moderate, medium angular blocky structure; many, medium, distinct, strong brown (7.5YR 4/6) iron and manganese redoximorphic features ; common, fine to medium roots; gravels are 10 to 15% by volume and range from 2 to 64+ mm with an average diameter of 8 mm; clear, wavy boundary.

Unit 6b:Bw2 (185-220 cm) is a brown (7.5YR 5/3), firm, gravelly clay with moderate, medium, angular blocky structure; common, medium, distinct strong brown redoximorphic features (7.5YR 4/6); increase in gravel size and abundance with 15 to 20% gravels by volume and a range from 2 to 64+ mm in diameter, with an average of 16 mm; decrease in root presence to few, fine to medium roots; abrupt, irregular boundary.

Unit 6a:(220-240 cm) is a dark, grayish brown (10YR 4/1), clayey gravel with platy bedding planes; clast supported imbrication; few, fine, distinct strong brown

redoximorphic features (7.5YR 4/6); no roots; limestone at >80%; abrupt, irregular boundary.

4.7.3 Interpretation

Unit 6a-c was deposited following a period of stability in the area indicated by the soil development of Unit 5. Following the period of stability and soil formation during the late Pleistocene, a high-energy stream channel event downcut into the Coats-Hines stratigraphy, eroding Units 2 through 5 along the drainage and depositing Unit 6a-c, which is composed of fluvial gravels that eroded from upland slopes (Figure 23 and 24). Poorly sorted pebble to cobble-size rock fragments dominate the channel units, primarily being composed of limestone and chert fragments. The gravels of Unit 6a exhibit clast-supported imbrication parallel to the east-west flow of the channel waters. Unit 6b and 6c do not exhibit imbrication instead are poorly sorted gravels and clay that were deposited from a combination of both the bed load and suspended load sediments rapidly falling out of suspension. A brief period of stability followed the deposition of Unit 6a-c, allowing for weak soil structure to develop in Unit 6b and 6c. The base of the unit (Unit 6a) rests on an unconformable contact with the oxidized clay of Unit 1. Similarly, Unit 6c was eroded along with Unit 5 before the deposition of Unit 7a-c (Figures 23 and 24).

COATS-HINES SITE (40WM31) LOCALITY I: DRAINAGE CHANNEL

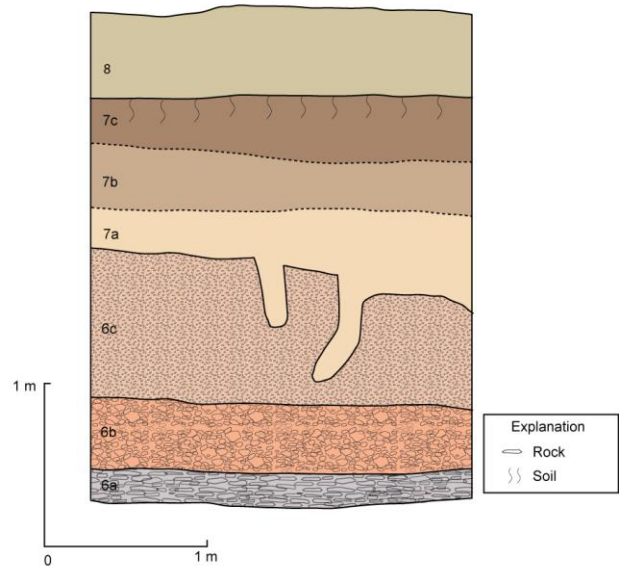


Figure 23. Locality I profile of channel unconformity.

COATS-HINES SITE (40WM31) LOCALITY II: DRAINAGE CHANNEL

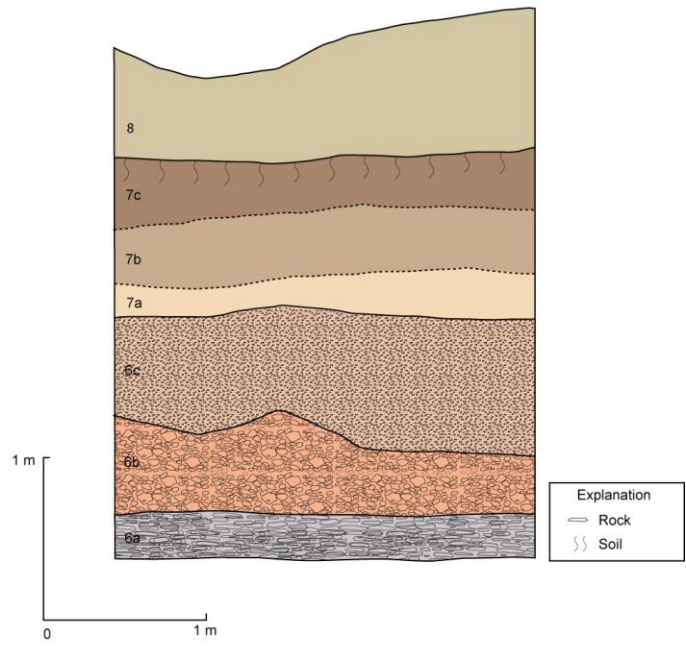


Figure 24. Locality II profile of channel unconformity.

4.8 Geochronology

The Coats-Hines site is located beyond glacial and periglacial conditions and given its position, was subject to higher insolation and moister conditions than more northern latitudes during the full-glacial period (Bettis et al. 2008). The high sediment and water discharge avulsion events that occurred at the site were the result climatic shifts. There are no obvious parallels between glacial outwash induced base level changes of the drainage, and therefore the periods of aggradation, erosion, and stability occurring at the site are likely the function of local climate (Brakenridge 1981).

The presence of limestone and chert fragments, ranging from weathered to freshly eroded indicate that the source is locally derived from the limestone bedrock upslope (Driese et al. 2005). Units 1 through 5 are largely the product of different episodes of colluvial/alluvial deposition from the nearby hillslopes during the late Pleistocene (Figure 25). The top of Unit 1 dates to $30,620 \pm 240^{14}\text{C}$ yr BP (UCIAMS-120335) and is a gravelly, heavily oxidized paleosol that was deposited during a particularly high energy episode of deposition. The gravel content in the lower Pleistocene units fine-upward indicating that the units following Unit 1 were deposited under such high energy and/or the bedrock exposure upslope became less exposed to weathering. After a brief period of stability in which soil structure was developed in Unit 1, Unit 2 was deposited between $26,310 \pm 150^{14}\text{C}$ yr BP (UCIAMS-120334) and $30,740 \pm 240^{14}\text{C}$ yr BP (UCIAMS-120333). The boundary between Unit 2 and Unit 1 is abrupt, indicating that Unit 1 was slightly eroded before Unit 2 was deposited directly on top of the surface. Unit 3 was deposited shortly after the deposition of Unit 2, dating to

26,290 ± 150 ¹⁴C yr BP (UCIAMS-120330). Again, Unit 3 was deposited on top of Unit 2 after pedogenesis occurred. The boundary between Unit 2 and 3 is abrupt, and therefore somewhat erosional. The base of the Unit 4 paleosol was deposited by 22,490 ± 100 ¹⁴C yr BP (UCIAMS-120329), following a period of stability and pedogenesis in Unit 3. Before Unit 4 was deposited, trees in the area fell, created discontinuous, mixed and convoluted bedding in Units 1, 2, and 3. Unit 4 was deposited on a flat-lying surface, after erosion had smoothed the surface of the treethrow features. The Pleistocene sediments are capped with Unit 5 which was likely deposited, shortly after Unit 4. The boundary between Unit 4 and 5 is abrupt and erosional. Given the thickness and extent of soil development in the lower Units, there was a long period of upland stability in the region.

Although Units 1, 2, 3, 4, and 5 are all part of the Pleistocene glacial package, they are separated by erosional contacts, indicating that before each period of aggradation in the lower units, there were brief periods of stability in which soil structure developed (Figure 25). Following the final Pleistocene aggradation, occurring around to 22,490 ± 100 ¹⁴C yr BP (UCIAMS-120329), there was a period of stability in which illuvial clays continued to accumulate in the lower units. The low chroma of Units 2, 3, and 4 in the lower profile of the excavation area signify that the paleosols formed under aquatic or semiaquatic conditions from fluctuations in the water table (Figure 25). Reduction represents anaerobic conditions caused by minimal permeability of the soil, preventing water from moving through the unit. Since the water can no longer move by means of gravitational or capillary flow, it becomes ponded. Such is the case in Unit 2,

3, and 4. In addition Units 1 through 5 contain Pleistocene faunal remains, including turtle fragments, again indicating saturated conditions. During the Pleistocene time period, the region was cool and wet, with the flora being dominated by boreal forest composed primarily of spruce (*Picea*) and pine (*Pinus*) (Delcourt 1979).

The Pleistocene-Holocene transition at the site area maintained a wet/humid climate with gradual warming (Alley and Clark 1999). The vegetation shifted from a boreal forest to a mixed boreal-deciduous forest composed of pine, spruce, and oak (Delcourt 1979). The change in vegetation along with the shift in climate may have caused the rapid downcutting and aggradation of channel deposits along the drainage. Unit 6a-c was deposited following a long period of stability in the area indicated by the soil development of the lower Pleistocene Units. Following the period of stability and soil formation during the late Pleistocene, a high-energy avulsion event downcut into the Coats-Hines stratigraphy, eroding Units 2 through 5 along the drainage and depositing Unit 6a-c, which is composed of fluvial gravels that eroded from upland slopes. Poorly sorted pebble to cobble-size rock fragments dominate the channel units, primarily being composed of limestone and chert fragments. The gravels of Unit 6a exhibit clast-supported imbrication parallel to the east-west flow of the channel waters. Unit 6b and 6c do not exhibit imbrication instead are poorly sorted gravels and clay that were deposited from a combination of both the bed load and suspended load sediments rapidly falling out of suspension. A brief period of stability followed the deposition of Unit 6a-c, allowing for weak soil structure to develop in Unit 6b and 6c. The base of the unit (Unit

6a) rests on an unconformable contact with the oxidized clay of Unit 1. Similarly, Unit 6c was eroded along with Unit 5 before the deposition of Unit 7a-c (Figure 25).

Unit 7a-c was deposited during the Holocene, when the region was warm and somewhat arid (Delcourt 1979). Deciduous hardwoods such as oak (*Quercus*) and hickory (*Carya*) were the dominant species of vegetation in the region (Delcourt 1979). Unit 7a-c is dominated by fine-grained sediment that chemically weathered from the limestone bedrock upslope. Unit 7a-c contain very little coarse fragments and therefore the sediments were likely transported under gradual, low-energy deposition rather than high-energy avulsion events like those occurring during the Pleistocene. No major climatic or biota shifts occurred in the region since 10,500 ¹⁴C yr BP in which a shift to fine-grained sedimentation dominated. After the sediments of Unit 7a-c were deposited there was a period of stability in which pedogenesis took place. Based on regional correlation which will be discussed in the following chapter, sedimentation during the Holocene ceased between 4000 and 2600 ¹⁴C yr BP, thus Unit 7a-c was deposited during the early to mid-Holocene.

Unit 8 was likely deposited during historic times, within the last few hundred years. The climate in the area has been consistent in the area for the past 4000 years; therefore it was not a climatic shift that caused the sedimentation of Unit 9. Given the lack of soil development, the deposition of Unit 8 was relatively recent. Relief and parent material hold constant and the deposition was not the result of climate, Unit 8 was likely deposited beginning in the 19th century when people began to occupy the area, farm and construct buildings. The construction and deforestation of the hill slopes

changed the stability of the sediment along the slopes, depositing silty clay loam at the site. Unit 8 would still be an active depositional surface if it was not buried by the modern backfill of Unit 9. Unit 9, as previously mentioned is modern backfill deposited within the last five to 10 years.

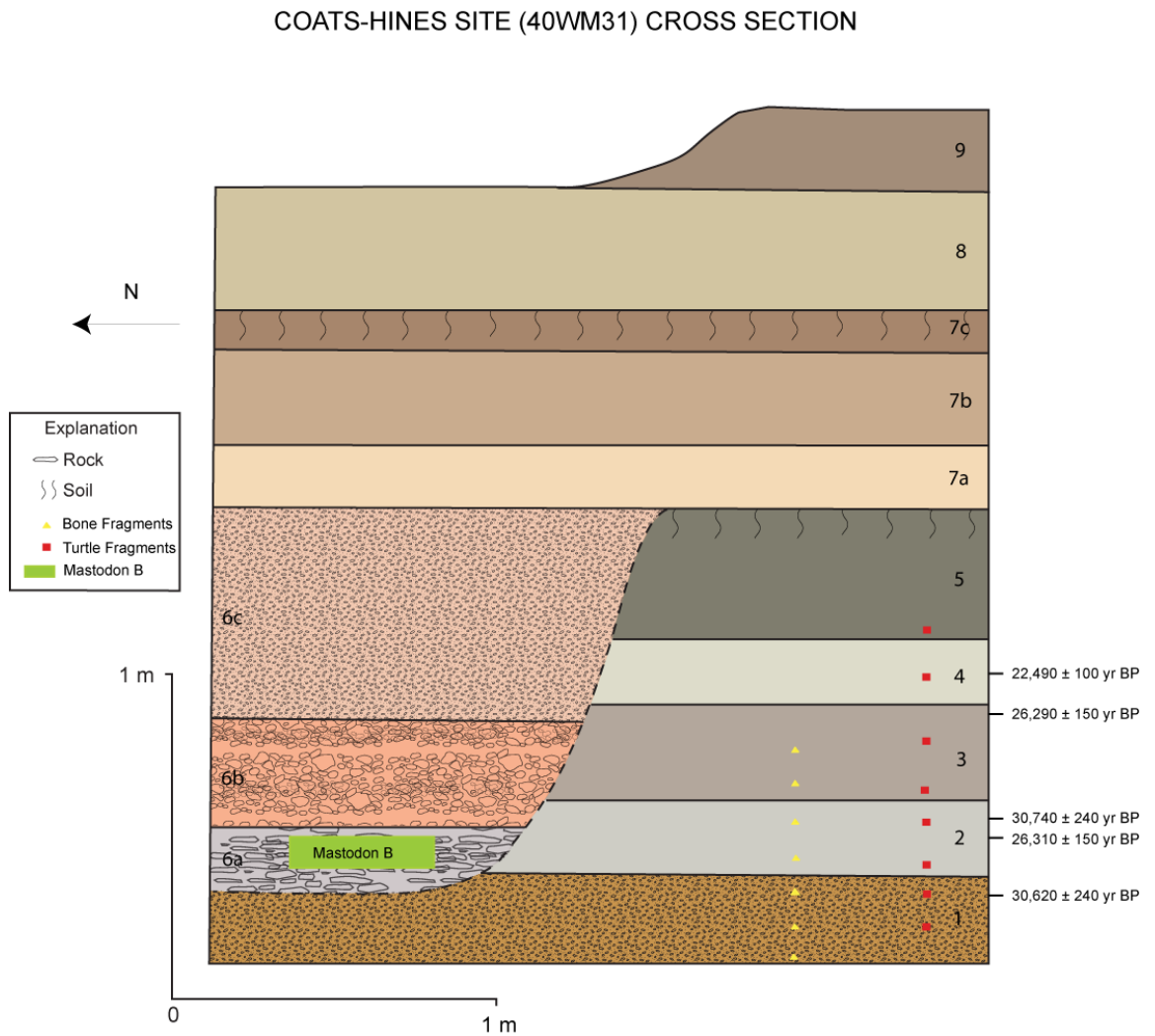


Figure 25. Generalized cross-section of the lithologic units at Coats-Hines.

CHAPTER V
CORRELATIONS

5.1 Introduction

The stratigraphic sequence of the Coats-Hines site has been correlated with the stratigraphy of the Duck River, the Pomme de Terre, and Douthard Creek (Figure 26). The sites were selected for correlation based on their location near the Coats-Hines site, in addition to all being south of glacial and periglacial conditions, therefore periods of lateral and vertical accretion are likely the result of climate shifts. The dates of deposition and stability are going to vary slightly based on location and variations in regional climate. Similarly, the composition and thickness of the stratigraphic units will vary based on source and energy of deposition (Appendix G).

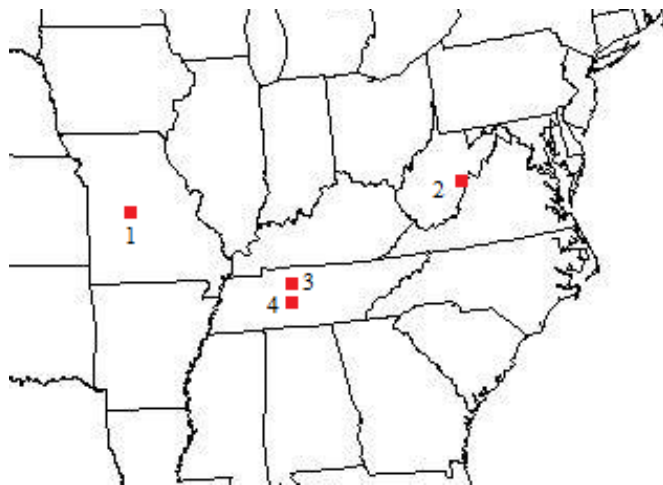


Figure 26. Study areas of the (1) Pomme de Terre River, Missouri; (2) Douthard Creek, West Virginia; (3) the Coats-Hines site, Tennessee; and (4) Duck River, Tennessee.

5.2 The Duck River, Tennessee

The Duck River is a meandering, northwesterly flowing meandering perennial stream located just 40 miles south of the Coats-Hines site. Brakenridge (1984) essentially defines three chronostratigraphic terrace sequences along the Duck River ranging from the late Pleistocene to modern deposition. Terrace 2 is the oldest terrace defined in the stratigraphy, and although no radiocarbon dates were collected, Brakenridge (1984) estimates the deposition to have occurred between 33,000 and 14,000 ^{14}C yr BP. Following the deposition of Terrace 2 there was a period of stability and soil development before several depositional events occurred through the Pleistocene-Holocene transition and the early to middle Holocene (Brakenridge 1984). Terrace 1 rests unconformably on top of Terrace 2 and was deposited in various stages beginning roughly 12,000 ^{14}C yr BP, and persisting until roughly 2600 ^{14}C yr BP (Brakenridge 1984). The composition shifts from a yellowish-brown clay loam in Terrace 2 to a brown silty loam of Terrace 1. A period of stability that coincided with the warmer, drier climate of the Holocene persisted until the historic period, in which the Duck River began to avulse and deposit modern silt and sandy loam of Terrace 0 (Brakenridge 1984). The sediments of Terrace 0 began being deposited in AD 1820 and continue today, with absence of pedogenic structure (Brakenridge 1984).

5.3 The Pomme de Terre River, Missouri

The Pomme de Terre River is a meandering northward-flowing perennial stream located in southern-central Missouri (Brakenridge 1981). Like the Coats-Hines site, the Pomme de Terre was never glaciated (Brakenridge 1981). Unlike the Coats-Hines site,

the Pomme de Terre has an alluvial history that dates back to 140,000 yr BP, although during the late Pleistocene, the Pomme de Terre has contains dated stratigraphic units that are remarkably similar to those of Coats-Hines (Brakenridge 1981). The Boney Spring formation of the Pomme de Terre is composed of two sedimentologically distinct members. The lower member of the formation is composed of olive/dark organic clay that was deposited beginning between 31,880 and 30,880 ^{14}C yr BP and ended by 22,000 ^{14}C yr BP. The upper member of the Boney Spring formation is composed of light gray to yellow-gray mottled clay that was deposited between 22,000 and 13,550 ^{14}C yr BP (Brakenridge 1981). The upper and lower members of the Boney Spring formation are not separated by an unconformity (Brakenridge 1981). The Boney Spring formation was followed by a period of stability and soil formation before Holocene aggradation beginning $10,200 \pm 330$ ^{14}C yr BP (Brakenridge 1981). Periodic deposition of the Holocene-age, Rodgers formation persisted, depositing fine-grained clayey silt until 1680 ± 100 ^{14}C yr BP, when once again, a period of stability and soil formation occurred (Brakenridge 1981). The final package along the Pomme de Terre is the historic, Pippens formation, which is composed of silty sand, and began its deposition as early as 840 ± 60 ^{14}C yr BP and continues to the present without evidence of pedogenic processes (Brakenridge 1981).

5.4 Douthard Creek, West Virginia

The floodplain-terrace system along the floodplain of Douthard Creek in southeastern West Virginia contains three distinct periods of deposition associated with climatic shifts occurring during the late Pleistocene and Holocene periods (Driese et al.

2005). The deposition along Douthard Creek is very similar to the deposits at the Coats-Hines site. The earliest stratigraphic package, called the Douthard paleosol, is a fine to medium silt and clay paleosol containing four gleyed B horizons with root traces and clay and iron hypocoatings underlain by a shale and gravel body. The deposition of the Douthard paleosol occurred during the late Pleistocene, persisting until $22,940 \pm 150$ ^{14}C yr BP (Driese et al. 2005). The Douthard paleosol formed under aquic conditions because of a fluctuating water table. This Pleistocene package also contains late Pleistocene flora and fauna and has a fining upward sequence of gravels indicating a colluvial/fluvial deposition. The Douthard paleosol is overlain unconformably by the Holocene 1 terrace, which is a weak soil and gravel rich horizon and the product of fluvial deposition. The deposition of the Holocene 1 terrace occurred as a result of the changing climate during the Pleistocene-Holocene transition. The upper portion of this terrace dates to 6360 ± 40 ^{14}C yr BP (Driese et al. 2005). Finally, Holocene Terrace 2 soil is defined as a modern surface soil, consisting of a fine sandy loam with two argillic B horizons and a sharp erosional contact at its base that dates to 3840 ± 40 ^{14}C yr BP (Driese et al. 2005).

5.5 Interpretation

All four sites experienced depositional events leading to vertical aggradation of sediment during the last glacial period, beginning roughly $30,000$ ^{14}C yr BP and ending by $22,000$ ^{14}C yr BP followed by a period of stability and soil development (Figure 27). The climate in these areas during the late Pleistocene was cool and wet, with boreal forests predominately being composed of pine (*Pinus*) and spruce (*Picea*) (Delcourt

1979; Alley and Clark 1999). The late Pleistocene deposits are generally composed of gravelly silts and clay, with higher clay content than the Holocene units preceding them. In addition, the redoximorphic features found in the late Pleistocene units of these areas indicate saturated conditions that were the result of a wet climate.

If the correlations between Coats-Hines and the selected sites during the Pleistocene, then one can correctly assume the correlation between sites during the Pleistocene-Holocene transition, and the Holocene (a period in which no dates were collected at the Coats-Hines site). The sites all have a unit/terrace that was deposited during the Pleistocene-Holocene transition, beginning between 14,000 and 10,000 C14 yr BP (Bettis et al. 2008). In the Southeast, the climate during this transition period was warm and wet with a mixed (Miller and Gingerich 2013) By roughly 4000 ¹⁴C yr BP, the climate was similar in the Southeast region to modern times (Delcourt 1979; Brakenridge 1984).

Unit 7a-c correlates with the brown, silt-rich early to middle Holocene alluvium mapped and dated along the Duck River, Pomme de Terre, and Douthard Creek (Figure 27). This silty fill is common to many sequences within Tennessee and the Southeast region (Brakenridge 1984).

Finally, the historic alluvial units of the Pomme de Terre correlate with Unit 8 of the 2012 excavation, with both being dominated by fine-grained sediment that has yet to develop soil structure (Figure 27). The Duck River also contains dark grayish-brown sediment that dates to a similar historic age as the Pomme de Terre River (Brakenridge 1981).

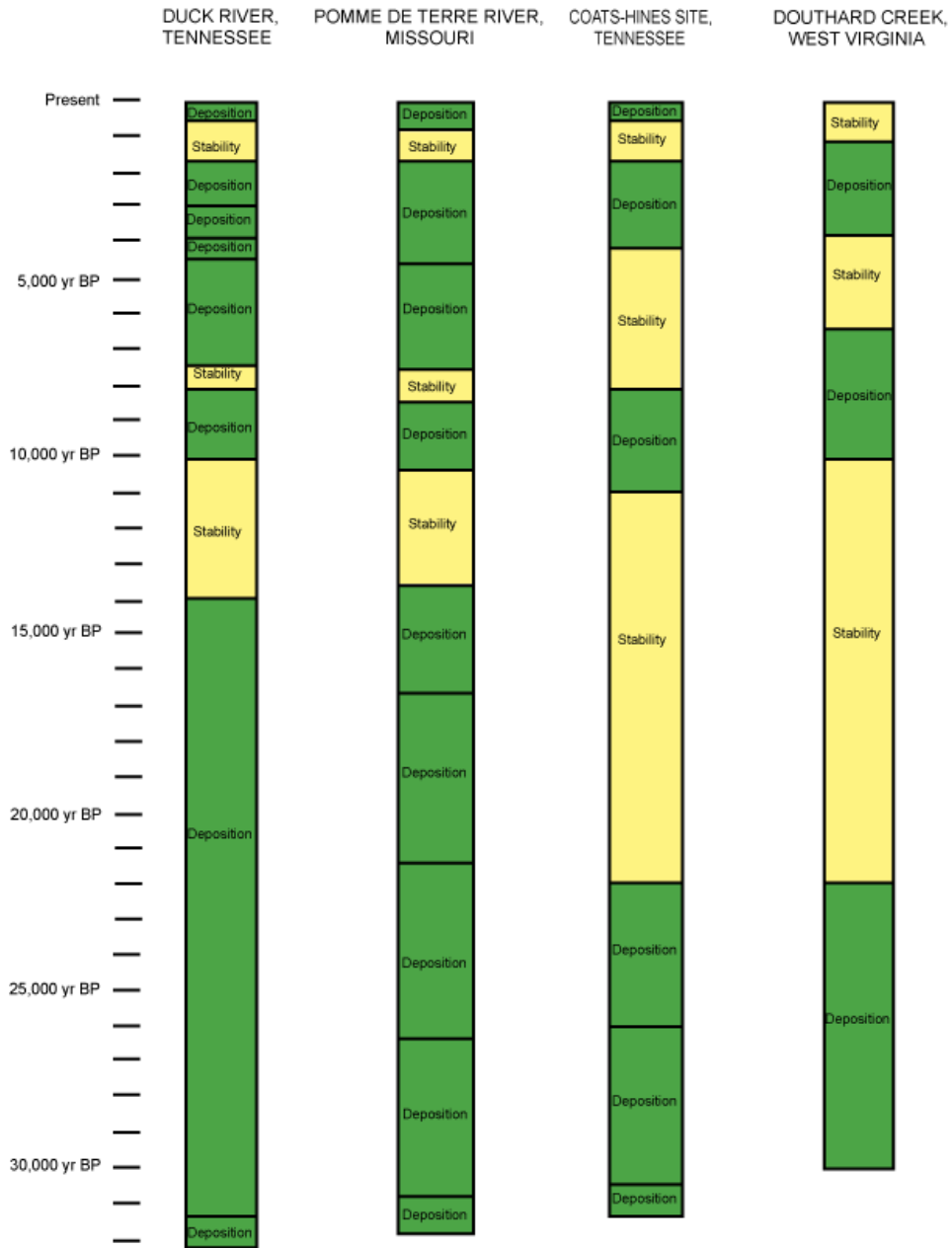


Figure 27. Time correlations of deposition and stability between the Duck River, Pomme de Terre River, Coats-Hines site, and Douthard Creek.

CHAPTER VI

ARCHAEOLOGICAL CONTEXT

6.1 Correlations of the 2012 Excavation to Previous Excavations at Coats-Hines

The 1994-1995 stratigraphic profile was completed by recording the general cross-section of the stratigraphic units along the drainage. The southern corner of the 1994-1995 connected with the northern wall of the 2012 pit. The stratigraphy between the northern wall and the 1994-1995 profile correlate well, with the designated bone bed of Mastodon B associating with Unit 2 of the 2012 pit. The dates from Unit 2 are too old to explain the deposits of the 1994-1995 excavation and given the methods of recording during the 1994 excavation, an unconformity was likely missed. Note, when comparing the profiles of the 1994-1995 excavation (Figure 3), the ground surface was lower by comparison to the 2010 test trench and 2012 excavation area due to the lack of modern backfill on the surface of the profile. The depth of the modern backfill is variable based on location (the site is slightly sloping towards the north) and date. Erosional processes dispersed the backfill downslope between the 2010 and 2012 excavation, making the backfill package thinner during the 2012 excavation.

The 2010 test trench intersects the 2012 excavation along the west wall; therefore the stratigraphy is the same between the two excavations (Table 4). Unit I of the 2010 trench is the same as Unit 8 and 9 of the 2012 excavation. Units II and III of the 2010 trench is actually the Holocene paleosol (Units 7a-c) recorded in 2012. Unit IV recorded in 2010 as a distinct dark gray clay loam is the silty clay paleosol of Unit 5. Unit V of the 2010 trench incorporates the Pleistocene paleosols of Units 4, 3, 2, and 1.

Table 4. Correlation between the stratigraphic units of the 2010 and 2012 excavations.

Stratigraphic Correlation with 2010 Test Trench	
2012 Geologic Units	2010 Geologic Units
9	Ia
8	Ib
7a-c	II, III
5	IV
4	Va
3	Va
2	Vb
1	Vb

6.2 Context of Mastodon B

Only Pleistocene faunal remains were discovered during the 2012 excavation. Similarly the 2010 trench stratigraphy is a match to the stratigraphy described and dated in the 2012 excavation pit, therefore the units of the 2010 excavation that were believed to contain archaeological remains precede the occupation of the Americas by several thousand years. The artifacts discovered during to 2010 excavation are geofacts, composed of chert that was weathered and broken through natural transportation processes. In addition, the ten lithic artifacts discovered during the 2010 excavation lack features typically associated with tool production, such as bulbs of percussion, striking platforms, ripple marks, etc.

Details regarding the context, stratigraphy, and association of the 1977 mastodon were never published and therefore this study will not be making any correlation to those finds. In addition, it was never stated whether the Area A Mastodon was discovered with artifacts to associate past human exploitation. In summary, this project will analyze the

deposition and context of the 1994-1995 mastodon remains and their association with lithic artifacts.

The plan view of the bone bed exposed during the 1994 excavation shows that the long bones are imbricated parallel to flow (Figure 28). Although the remains of Mastodon B are disarticulated they are in close proximity indicating that they are near their primary context but slightly transposed.

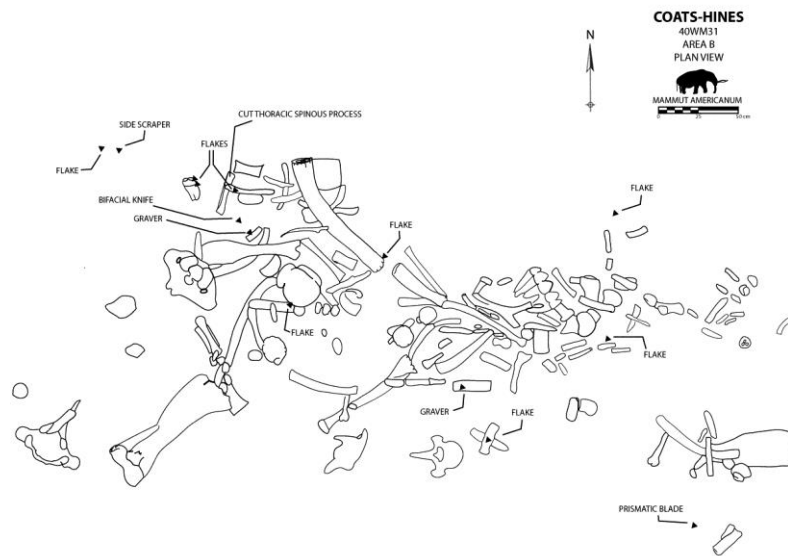


Figure 28. Planview of Mastodon B (Breitburg et al. 1996).

Breitburg and Broster (1995) recorded the mastodon and lithic artifacts to be located in blue/gray clay (Figures 3 and 25). The channel sediment of Units 6b and 6c are mottled with oxidized iron and manganese. Unit 6a is a dark, grayish brown deposit. Mastodon B could have been discovered resting on top or within Unit 6a, becoming rapidly buried and preserved by the gravelly clays of Unit 6b and 6c.

In addition, the 1994-1995 excavation recorded the stratigraphy of the drainage cross section for every 2.5 m, claiming that the stratigraphic units were deposited on smooth, horizontal beds. The 1994-1995 excavation also recorded heavy mixing due to the turbation from worms and tree roots of redistributing and creating poor sorting of large gravels within the cross section. The bioturbation was not recorded in the profile and upon inspection of photographs of the excavation, no worm burrows or tree root turbation are visible. Similarly, is not possible for worms to disrupt the sorting of larger clast materials in the stratigraphy. Instead, the most likely scenario is that the mastodon was deposited on the surface of the gravel thalweg of the channel unconformity and rapidly buried by poorly sorted clays and gravels during the Pleistocene-Holocene transition. The channel containing Units 6a-c is very narrow and given that the cross section was investigated on such a large scale, rather than following discrete units and contacts, the channel unconformity could have been missed. The mixing of large cobbles with clay also represent a high energy flow, the bulk sediment was deposited contemporaneously without sorting based on weight or cohesion, likely during a flood event. Given that the bottom of the channel unconformity contains large cobbles (32 to 64+ mm) that are also oriented parallel to stream flow, it is likely that Mastodon B was buried early in the flood event and in or near its original context (Figure 25).

Additional evidence of the Pleistocene-Holocene association of Mastodon B (compared to the 30,000 to 22,000 ^{14}C year old dates of Unit 2) is given by the amount of iron replacement in the bones. Many of the larger bones excavated within the 2012 pit as well as in the 2010 trench were heavily replaced/impregnated with iron oxide (Deter-

Wolf et al. 2011). Mastodon B does not have any staining/replacement/impregnation of minerals due to the differing depositional context and environment from the older deposits.

No charcoal dates were collected during the March 2013 survey to definitively state the antiquity of the deposits, but the organic sediment of the channel will be dated in the future, along with potential dates obtained from the bone of Mastodon B.

CHAPTER VII

CONCLUSION

The Coats-Hines site (40WM31) is a Clovis or potential pre-Clovis Mastodon site located in northern Williamson County, Tennessee. The site rests along the convergence of the Central Basin and Western Highland Rim. The Coats-Hines site was discovered during the construction of a nearby golf course when a salvage team uncovered a mature female mastodon. The site was later excavated in 1994-1994, during which time two additional mastodons were uncovered, in direct association with lithic artifacts. Preliminary radiocarbon dates reveal the site was deposited during the late Pleistocene epoch at roughly 12,000 ^{14}C yr BP (Breitburg et al. 1996).

During the summer of 2012, the site was excavated by Texas A&M University with the goal of determining the stratigraphy and depositional setting of the site as well as establishing the antiquity of the archaeological remains through investigation of the depositional history and context of the lithic and faunal remains. The site geology was determined through field interpretation and hand-texturing, micromorphological analysis, laboratory particle size analysis, and radiocarbon dating. Sedimentation at the site is a combination of cherty colluvium from upslope as well as alluvium. Four chronostratigraphic sequences of sedimentation were determined to have occurred during the last glacial, the Pleistocene-Holocene transition, the Holocene, and historic-modern time periods. The volume, distribution, and composition of the nine defined stratigraphic units are dependent on the fluctuations occurring in the climate during these

time periods. The climate changes and rates of deposition occurring at Coats-Hines were correlated to similar sites in the region.

This study has identified four different geochronological groups separated into nine different lithologically distinct units. Radiocarbon dates from Units 1 through 4 in the excavation area were collected, placing the lower deposits of the 2012 excavation in the last glacial period of the late Pleistocene (between $31,140 \pm 270$ and $22,490 \pm 100$ ^{14}C yr BP). Following the Spring 2013 Coats-Hines site survey along the wet-weather drainage a channel unconformity was discovered, likely dating to the Pleistocene-Holocene transition based on correlation to regional stratigraphy. The Pleistocene-Holocene channel provides context to the mastodon and lithic remains discovered along the drainage during the 1994-1995 excavation. Finally, both the channel and the Pleistocene sediments were buried by fine-grained Holocene sediment deposition.

REFERENCES

- Alley, Richard B. and Peter U. Clark
1999 The Deglaciation of the Northern Hemisphere: A Global Perspective. *Annual Reviews of Earth and Planetary Sciences* 27: 149-182.
- Bettis, E. Arthur III, David W. Benn, and Edwin R. Hajic
2008 Landscape Evolution, Alluvial Architecture, Environmental History, and the Archaeological Record of the Upper Mississippi River Valley. *Geomorphology* 101: 362-377.
- Brakenridge, G. Robert
1981 Late Quaternary Floodplain Sedimentation along the Pomme de Terre River, southern Missouri. *Quaternary Research* 15(1):62-76.
- 1984 Alluvial Stratigraphy and Radiocarbon Dating along the Duck River, Tennessee: Implications Regarding Floodplain Origin. *Geological Society of America Bulletin* 95(1): 9-25.
- Breitburg, Emmanuel and John B. Broster
1995 A Hunt for Big Game: Does Coats-Hines Site Confirm Human/Mastodon Contact?. *The Tennessee Conservationist* 61(4): 18-26.
- Breitburg, Emmanuel, John B. Broster, Arthur L. Reesman, and Richard Stearns
1996 The Coats-Hines Site: Tennessee's First Paleoindian-Mastodon Association. *Current Research in the Pleistocene* 13: 6-8.
- Brewer, R., and J.R. Sleeman
1988 *Soil Structure and Fabric*. CSIRO Division of Soils, Adelaide, Australia.
- Delcourt, Hazel R.
1979 Late Quaternary Vegetation History of the Eastern Highland Rim and Adjacent Cumberland Plateau of Tennessee. *Ecological Monographs* 49 (3): 255-280.
- Deter-Wolf, Aaron, Jesse W. Tune, and John B. Broster
2011 Excavations and Dating of Late Pleistocene and Paleoindian Deposits at the Coats-Hines Site, Williamson County, Tennessee. *Tennessee Archaeology* 5(2): 142-156.
- Driese, S.G., with Li, Z.-H., and Horn, S.P.
2005 Late Pleistocene to Holocene Paleoclimate and Paleogeomorphic History Interpreted from 23,000 14C yr B.P. Paleosol and Floodplain Soils, southeastern West Virginia, USA. *Quaternary Research* 63:136-149.

- Embleton-Hamann, Christine
 2004 Process Responsible for the Development of a Pit and Mound Relief. *Catena* 57: 175-188.
- Fitzpatrick, E.A.
 1984 *Micromorphology of Soils*. Chapman and Hall, New York.
 1993 *Soil Microscopy and Micromorphology*. John Wiley & Sons, New York.
- Guccione, Margaret J.
 2008 Impact of the Alluvial Style on the Geoarchaeology of Stream Valleys. *Geomorphology* 101: 378-401.
- Holliday, Vance T.
 2009 Geoarchaeology and the Search for the First Americans. *Catena* 78: 310-322.
- Kilmer, V. H., and L. Z. Alexander
 1949 Methods for Making Mechanical Analyses of Soil. *Soil Sci.* 68:15-24.
- Krumbein, W.C. and L.L. Sloss
 1963 *Geology, Stratigraphic; Sedimentation and Deposition*. 2nd edition. W.H. Freeman, San Francisco.
- Miller, Shane D. and Joseph A.M. Gingerich
 2013 Regional Variation in the Terminal Pleistocene and Early Holocene Radiocarbon Record of eastern North America. *Quaternary Research* 79: 175-188.
- Rapp, George, and Christopher L. Hill
 2006 *Geoarchaeology: The Earth-Science Approach to Archaeological Interpretation*. 2nd edition. Yale University Press, New Haven, CT.
- Reesman, A.L., and Stearns, R.G. 1989. The Nashville dome – An Isostatically Induced Erosional Structure – and the Cumberland Plateau Dome – an Isostatically Suppressed Extension of the Jessamine Dome. *Southeastern Geology*, 30:147-174.
- Schaetzl, Randall, and Sharon Anderson
 2005 *Soils: Genesis and Geomorphology*. Cambridge University Press, Cambridge, England.
- Stoops, Georges
 2003 *Guidelines for Analysis and Description of Soil and Regolith Thin Sections*. Soil Science Society of America, Inc., Madison, WI.

Waters, Michael R.

1992 *Principles of Geoarchaeology: A North American Perspective*. The University of Arizona Press, Tucson.

Whitehouse, David

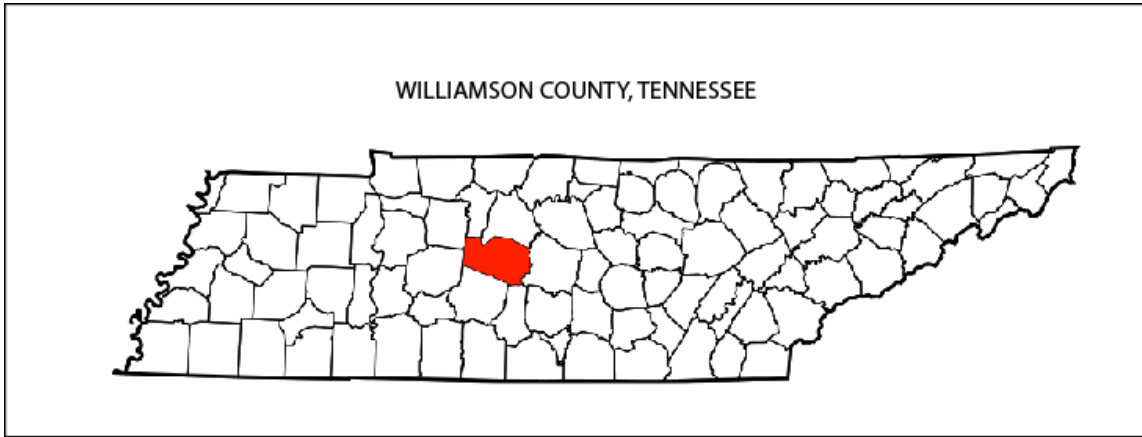
2004 *Surfaces and their Measurement*. Kogan Page Science, London.

Wilson, Charles W. and Robert A. Miller

1963 *Geologic Map of the Franklin Quadrangle, Tennessee*. Tennessee Valley Authority, Nashville.

APPENDIX A

WILLIAMSON COUNTY, TENNESSEE



APPENDIX B
PIPPETTE ANALYSIS

ID	DEPTH (cm)	PARTICLE SIZE DISTRIBUTION (mm)										TEXTURE CLASS	COARSE FRAG- MENTS %	
		-----SAND-----					-----SILT-----		-----CLAY-----					
		VC	C	M	F	VF	TOTAL	FINE	TOTAL	FINE				TOTAL
		(2.0- 1.0)	(1.0- 0.5)	(0.5- 0.25)	(0.25- 0.10)	(0.10- 0.05)	(2.0- 0.05)	(0.02- 0.002)	(0.05- 0.002)	(<0.0002)				(<0.002)
-----%-----														
Unit 8	20-30	0.3	0.5	0.7	3.5	6.0	11.0	40.0	63.1	9.2	25.9	SiL		
Unit 8	30-40	0.5	0.4	0.6	4.2	6.9	12.6	34.9	58.4	11.7	29.0	SiCL		
Unit 8	40-50	0.1	0.3	0.4	2.2	4.6	7.6	36.0	58.1	14.8	34.3	SiCL		
Unit 8	50-60	0.6	0.8	1.2	3.4	3.7	9.7	41.2	60.1	10.7	30.2	SiCL		
Unit 8	60-66	0.5	0.8	1.2	3.3	3.4	9.2	43.3	61.9	9.6	28.9	SiCL	1	
Unit 7c	66-70	0.4	0.6	0.8	2.8	2.9	7.5	48.7	66.2	7.1	26.3	SiL		
Unit 7c	70-80	0.3	0.6	0.8	2.4	2.6	6.7	48.4	64.2	8.3	29.1	SiCL		
Unit 7b	80-90	0.4	0.5	0.7	2.3	2.4	6.3	44.6	60.3	12.3	33.4	SiCL		
Unit 7b	90-100	0.3	0.5	0.6	2.1	2.3	5.8	42.4	56.3	16.9	37.9	SiCL		
Unit 7b	100-110	0.7	0.4	0.6	2.1	2.2	6.0	43.9	56.9	17.5	37.1	SiCL		
Unit 7a	115-120	0.5	0.7	0.7	2.8	2.4	7.1	42.1	56.6	18.1	36.3	SiCL		
Unit 7a	120-130	0.5	0.7	0.7	2.9	2.3	7.1	41.7	55.3	19.7	37.6	SiCL		
Unit 7a	130-140	0.5	0.5	0.5	2.7	2.2	6.4	39.3	52.4	23.3	41.2	SiC		
Unit 5	140-150	0.2	0.3	0.3	1.6	1.4	3.8	36.3	47.8	26.8	48.4	SiC		
Unit 5	150-160	0.0	0.1	0.1	0.8	1.0	2.0	41.2	52.5	22.4	45.5	SiC		
Unit 5	160-170	0.1	0.2	0.1	0.9	0.9	2.2	43.4	56.8	19.0	41.0	SiC		
Unit 5	170-180	0.7	0.7	0.3	1.1	1.0	3.8	41.6	55.3	18.7	40.9	SiC		
Unit 5	180-190	0.1	0.2	0.2	1.1	1.1	2.7	44.5	59.7	17.6	37.6	SiCL		
Unit 4	190-200	0.1	0.1	0.2	2.1	2.4	4.9	40.9	55.4	23.2	39.7	SiCL		
Unit 4	200-210	0.1	0.1	0.2	2.7	2.8	5.9	39.7	53.6	25.0	40.5	SiC		
Unit 4	210-220	0.2	0.2	0.4	4.3	3.5	8.6	36.7	52.2	24.2	39.2	SiCL		
Unit 3	220-230	0.4	0.5	0.7	5.3	4.4	11.3	34.6	49.2	22.9	39.5	SiCL	1	
Unit 3	230-240	0.8	0.6	0.8	6.5	5.3	14.0	33.1	48.4	20.8	37.6	SiCL	1	
Unit 3	240-250	0.8	0.6	1.0	6.9	4.9	14.2	30.6	44.8	24.0	41.0	SiC	1	
Unit 2	250-260	0.8	0.6	1.1	8.5	6.2	17.2	28.1	38.6	27.3	44.2	C	2	
Unit 2	260-270	0.6	0.6	1.1	8.6	6.4	17.3	27.4	37.3	28.3	45.4	C	1	
Unit 1	270-280	2.0	1.4	1.8	8.6	6.5	20.3	23.5	33.7	26.0	46.0	C	6	
Unit 1	280-290	1.6	1.4	1.5	7.9	5.9	18.3	25.3	35.6	24.9	46.1	C	6	

APPENDIX C

STRATIGRAPHIC DESCRIPTIONS

Unit 9 (0-22 cm)	
Texture Class	Silt loam
Dry Consistence	Soft
Moist Consistence	Very friable
Munsell Color	Dry: 10YR 4/2 (brown); Moist: 10YR 3/3 (dark brown)
Plasticity	Slightly Plastic
Sedimentary structures (Type, Grade, Class)	Single grained; Fine, Structureless
Redox features	None
Boundaries/contacts	Clear; Smooth
Horizon designation	N/A: modern backfill
Special Features	N/A

Unit 8 (22-55 cm)	
Texture Class	Silty clay loam
Dry Consistence	Slightly hard
Moist Consistence	Friable
Munsell Color	Dry: 10YR 4/3 (brown); Moist: 10YR 4/4 (dark yellowish brown)
Plasticity	Plastic
Sedimentary structures (Type, Grade, Class)	Single grained; Fine, Structureless
Redox features	None
Boundaries/contacts	Clear; Smooth
Horizon designation	N/A: No soil structure
Special Features	N/A

Unit 7c (55-70 cm)	
Texture Class	Silty clay loam
Dry Consistence	Slightly hard
Moist Consistence	Friable
Munsell Color	Dry: 10YR 3/3 (dark brown); Moist: 10YR 2/2 (very dark brown)
Plasticity	Plastic
Sedimentary structures (Type, Grade, Class)	Granular; Moderate; Fine
Redox features	None
Boundaries/contacts	Clear; Smooth
Horizon designation	Ab
Special Features	N/A

Unit 7b (70-100 cm)	
Texture Class	Silty clay loam
Dry Consistence	Slightly hard
Moist Consistence	Friable
Munsell	Dry: 7.5YR 3/2 (brown); Moist: 7.5YR 3/3 (brown)
Plasticity	Plastic
Sedimentary structures (Type, Grade, Class)	Subangular blocky; Moderate; Fine
Redox features	Few; faint
Boundaries/contacts	Clear; Smooth
Horizon designation	Btb1
Special Features	Secondary accumulation of clay

Unit 7a (100-120 cm)	
Texture Class	Silty clay loam
Dry Consistence	Slightly hard
Moist Consistence	Friable
Munsell Color	Dry: 10YR 4/3 (brown); Moist: 10YR 4/2 (dark grayish brown)
Plasticity	Plastic
Sedimentary structures (Type, Grade, Class)	Subangular blocky; Moderate; Medium
Redox features	Few; faint
Boundaries/contacts	Abrupt; Smooth
Horizon designation	Btb2
Special Features	Clay coating on ped surfaces

6c (1.525-2.325m)	
Texture Class	Slightly gravelly clay
Dry Consistence	Hard
Moist Consistence	Firm
Munsell Color	Dry: 7.5YR 5/4 (brown); Moist: 7.5YR 4/4 (brown)
Plasticity	Plastic
Sedimentary structures (Type, Grade, Class)	Angular blocky; Moderate; Medium
Redox features	Many; Distinct
Boundaries/contacts	Clear; Wavy
Horizon designation	Bw1
Special Features	Clay coating on ped surfaces; Fe-Mn concentrations; Siliceous gravels

6b (2.325-2.825)	
Texture Class	Gravelly clay
Dry Consistence	Hard
Moist Consistence	Firm
Munsell Color	Dry: 7.5 YR 5/3 (brown); Moist: 7.5YR 5/4 (brown)
Plasticity	Plastic
Sedimentary structures (Type, Grade, Class)	Angular blocky; Moderate; Medium
Redox features	Common; Distinct
Boundaries/contacts	Abrupt; Irregular
Horizon designation	Bw2
Special Features	Clay coating on ped surfaces; Fe-Mn concentrations; Siliceous gravels

6a (2.825-3.075)	
Texture Class	Clayey Gravel (>80% gravel)
Dry Consistence	Hard
Moist Consistence	Firm
Munsell Color	Dry: 10YR 4/1 (dark grayish brown); Moist: 10YR 4/1 (dark yellowish brown)
Plasticity	Non-Plastic
Sedimentary structures (Type, Grade, Class)	Platy
Redox features	Few; Distinct
Boundaries/contacts	Abrupt; Wavy
Horizon designation	N/A
Special Features	Channel gravels

Unit 5 (120-160 cm)	
Texture Class	Silty clay
Dry Consistence	Hard
Moist Consistence	Firm
Munsell Color	Dry: 10YR 3/2 (very dark grayish brown); Moist: 10YR 3/3 (dark brown)
Plasticity	Plastic
Sedimentary structures (Type, Grade, Class)	Subangular blocky; Moderate; Fine
Redox features	Common; Distinct
Boundaries/contacts	Abrupt; Smooth
Horizon designation	2Btb
Special Features	Clay coating on ped surfaces; Fe-Mn concentrations; Siliceous gravels

Unit 4 (160-180 cm)	
Texture Class	Silty clay
Dry Consistence	Hard
Moist Consistence	Firm
Munsell Color	Dry: 10YR 4/2 (dark grayish brown); Moist: 10YR 4/4 (dark yellowish brown)
Plasticity	Plastic
Sedimentary structures (Type, Grade, Class)	Subangular blocky; Moderate; Medium
Redox features	Common; Distinct
Boundaries/contacts	Abrupt; Irregular
Horizon designation	2Btgb
Special Features	Clay coating on ped surfaces; Fe-Mn concentrations; Siliceous gravels

Unit 3 (180-210 cm)	
Texture Class	Silty clay
Dry Consistence	Hard
Moist Consistence	Firm
Munsell Color	Dry: 7.5YR 4/2 (brown); Moist: 10YR 4/4 (dark yellowish brown)
Plasticity	Plastic
Sedimentary structures (Type, Grade, Class)	Subangular blocky; Moderate; Medium
Redox features	Common; Prominent
Boundaries/contacts	Abrupt; Irregular
Horizon designation	2Btgb2
Special Features	Clay coating on ped surfaces; Fe-Mn concentrations; Siliceous gravels

Unit 2 (201-235 cm)	
Texture Class	Clay
Dry Consistence	Hard
Moist Consistence	Firm
Munsell Color	Dry: 10YR 5/1 (gray); Moist: 10YR 5/1 (gray)
Plasticity	Plastic
Sedimentary structures (Type, Grade, Class)	Subangular blocky; Moderate; Medium
Redox features	Few; Distinct
Boundaries/contacts	Abrupt; Irregular
Horizon designation	2Btgb3
Special Features	Clay coating on ped surfaces; Fe-Mn concentrations; Siliceous gravels

Unit 1 (235-260 cm)	
Texture Class	Slightly Gravelly Clay
Dry Consistence	Hard
Moist Consistence	Firm
Munsell Color	Dry: 7.5YR 4/6 (strong brown), Moist: 7.5YR 4/6 (strong brown)
Plasticity	Plastic
Sedimentary structures (Type, Grade, Class)	Subangular blocky; Moderate; Medium
Redox features	Many; Prominent
Boundaries/contacts	Abrupt; Irregular
Horizon designation	2Btg4
Special Features	Clay coating on ped surfaces; Fe-Mn concentrations; Siliceous gravels

APPENDIX D
GRAVEL ANALYSIS

Unit 996/1008																							
Level 51		Composition			Roundness										Sphericity								
Size (mm)	Weight (g)	Li me	Sa nd	Ch ert	0.1	%	0.3	%	0.5	%	0.7	%	0.9	%	0.3	%	0.5	%	0.7	%	0.9	%	
63	-	-	-	-	-	-	-	-	-	-	-	-	-	-	-	-	-	-	-	-	-	-	-
31.5	-	-	-	-	-	-	-	-	-	-	-	-	-	-	-	-	-	-	-	-	-	-	-
16	34.9	34.6	-	-	14.6	42.2	12.4	15.4	15.7	45.9	-	-	-	-	20.3	58.7	14.6	42.2	-	-	-	-	-
8	227.6	227.6	-	-	32.6	14.3	37.4	16.2	24.6	10.3	52.3	2.3	81.2	65.1	28.6	81.7	35.9	78.1	34.3	2.3	1.3	2.3	1.1
4	144.5	142.3	-	2.1	24.1	16.7	15.5	10.7	39.1	27.4	61.6	4.3	4.9	-	-	-	-	-	-	-	-	-	-
2	2.1	-	-	-	-	-	-	-	-	-	-	-	-	-	-	-	-	-	-	-	-	-	-
Totals	409.1	404.9	-	2.1	71.3	17.5	57.2	14.1	79.2	19.5	113.9	2.8	85.4	2.1	-	-	-	-	-	-	-	-	-
Level 52					Roundness										Sphericity								
Size (mm)	Weight (g)	Li me	Sa nd	Ch ert	0.1	%	0.3	%	0.5	%	0.7	%	0.9	%	0.3	%	0.5	%	0.7	%	0.9	%	
63	-	-	-	-	-	-	-	-	-	-	-	-	-	-	-	-	-	-	-	-	-	-	-
31.5	-	-	-	-	-	-	-	-	-	-	-	-	-	-	-	-	-	-	-	-	-	-	-
16	77.9	77.9	-	-	12.3	15.7	16.1	20.7	24.4	31.3	18.2	2.3	6.9	8.9	9.5	12.2	12.9	16.6	40.5	5.5	52.5	1.5	1.9
8	190.7	190.7	-	-	41.7	21.9	33.4	17.5	78.4	41.2	32.7	1.7	4.4	2.3	37.8	19.8	75.4	39.5	71.9	37.7	5.6	2.9	2.9
4	154.3	154.2	-	0.1	14.3	9.3	36.4	23.6	78.1	50.6	20.8	1.4	4.3	-	-	-	-	-	-	-	-	-	-
2	6.1	-	-	-	-	-	-	-	-	-	-	-	-	-	-	-	-	-	-	-	-	-	-
Totals	429	422.8	-	0.1	68.3	16.2	85.9	20.3	181.8	42.7	71.7	1.7	3.8	3.8	-	-	-	-	-	-	-	-	-
Level 53					Roundness										Sphericity								
Size (mm)	Weight (g)	Li me	Sa nd	Ch ert	0.1	%	0.3	%	0.5	%	0.7	%	0.9	%	0.3	%	0.5	%	0.7	%	0.9	%	
63	-	-	-	-	-	-	-	-	-	-	-	-	-	-	-	-	-	-	-	-	-	-	-
31.5	50.5	50.5	-	-	-	-	-	-	50.5	10.0	-	-	-	-	-	-	50.5	10.0	-	-	-	-	-
16	104.5	104.5	-	-	18.7	17.9	15.6	14.9	32.3	30.9	37.9	3.6	-	-	15.4	14.7	67.8	64.9	21.3	20.4	-	-	-
8	478.4	472.5	-	5.9	77.5	16.2	106.9	22.3	242.9	50.8	41.5	8.8	9.2	62.9	13.1	17.6	36.8	233.1	48.7	48.4	6.3	1.3	1.3
4	463.1	461.4	-	2.1	17.5	3.8	60.8	13.1	352.4	76.1	23.3	5.5	1.2	-	-	-	-	-	-	-	-	-	-
2	17.4	-	-	-	-	-	-	-	-	-	-	-	-	-	-	-	-	-	-	-	-	-	-
Totals	1113.9	1089.9	-	8	113.7	10.4	183.3	16.7	678.1	61.8	102.7	9.4	18.7	1.7	-	-	-	-	-	-	-	-	-

Level 54					Roundness										Sphericity								
Size (mm)	Weight (g)	Li me	Sa nd	Ch ert	0.1	%	0.3	%	0.5	%	0.7	%	0.9	%	0.3	%	0.5	%	0.7	%	0.9	%	
63	-	-	-	-	-	-	-	-	-	-	-	-	-	-	-	-	-	-	-	-	-	-	-
31.5	55.3	23.3	32.1	-	23.2	42	-	-	32.1	58	-	-	-	-	55.3	10	-	-	-	-	-	-	-
16	189	139.4	4.4	45.2	35.5	9	70.5	37.5	30.8	16.3	45.8	24	6.5	3.4	22.1	11.7	90.5	47.9	69.8	36.9	6.6	3.5	
8	637.3	599.1	-	38.2	72.6	11.4	137.4	21.6	344.9	54.1	75.3	12	7.1	1.1	91.6	14.4	227.6	35.7	303.7	47.5	9.1	1.4	
4	570.2	566.8	-	3.4	34.7	6.1	113.8	20.8	359.1	63.1	56.8	9	9.5	1	-	-	-	-	-	-	-	-	-
2	28.8	-	-	-	-	-	-	-	-	-	-	-	-	-	-	-	-	-	-	-	-	-	-
Totals	1480.6	132.9	36.5	86.8	165.5	11.4	322.1	22.2	767.6	52.9	177.1	12	19.5	1.3									
Level 55					Roundness										Sphericity								
Size (mm)	Weight (g)	Li me	Sa nd	Ch ert	0.1	%	0.3	%	0.5	%	0.7	%	0.9	%	0.3	%	0.5	%	0.7	%	0.9	%	
63	-	-	-	-	-	-	-	-	-	-	-	-	-	-	-	-	-	-	-	-	-	-	-
31.5	25.3	25.3	-	-	-	-	-	-	-	-	25.3	10	-	-	25.3	10	-	-	-	-	-	-	-
16	128	128	-	-	44.1	34.4	17.7	13.8	45.4	35.5	15.9	12	4.9	3.8	32.2	25.8	47.3	37.3	48.48	37.5	-	-	
8	450.1	441.9	-	8.2	76.1	16.9	70.9	15.8	211.8	47.1	85.8	19	6.4	1.4	72.9	16.2	168.7	37.5	204.2	45.4	14.5	3.2	
4	323.2	319.4	0.6	3.2	39.7	12.3	46.7	14.4	195.5	60.5	37.5	12	4.2	1	-	-	-	-	-	-	-	-	-
2	5.8	-	-	-	-	-	-	-	-	-	-	-	-	-	-	-	-	-	-	-	-	-	-
Totals	932.4	914.6	0.6	11.4	159.9	17.3	135.3	14.6	452.7	48.9	163.5	18	15.1	1.6									
Level 56					Roundness										Sphericity								
Size (mm)	Weight (g)	Li me	Sa nd	Ch ert	0.1	%	0.3	%	0.5	%	0.7	%	0.9	%	0.3	%	0.5	%	0.7	%	0.9	%	
63	-	-	-	-	-	-	-	-	-	-	-	-	-	-	-	-	-	-	-	-	-	-	-
31.5	-	-	-	-	-	-	-	-	-	-	-	-	-	-	-	-	-	-	-	-	-	-	-
16	354.6	328	9.5	17.1	45.7	12.9	80.2	22.6	178.5	50.3	44.4	13	8.6	6	44.3	12.5	124.3	35.1	112.1	31.6	73.9	2.1	
8	673.5	660.9	-	12.6	101.5	15.1	23.156	2.3	313.3	46.5	84.4	13	18.3	2.7	59.4	8.8	232.6	34.5	346.4	51.4	35.1	5.2	
4	511.5	508.6	-	2.9	49.1	9.6	60.7	11.9	319.6	62.4	69.4	14	12.5	2	-	-	-	-	-	-	-	-	-
2	18.1	-	-	-	-	-	-	-	-	-	-	-	-	-	-	-	-	-	-	-	-	-	-
Totals	1557.7	149.8	9.5	32.6	196.3	12.8	296.9	19.3	811.4	52.7	198.2	13	36.8	2.4									

Level 57					Roundness										Sphericity								
Size (mm)	Weight (g)	Li me	Sa nd	Ch ert	0.1	%	0.3	%	0.5	%	0.7	%	0.9	%	0.3	%	0.5	%	0.7	%	0.9	%	
63	-	-	-	-	-	-	-	-	-	-	-	-	-	-	-	-	-	-	-	-	-	-	-
31.5	82	82	-	-	-	-	35.	43	46.	56	-	-	-	-	35.	43	-	-	46.	56	-	-	-
16	436.9	334.6	-	102.3	11	25	81.	18	17	40	67.	1	0.	62	14	15	36	21	49	-	-	-	
8	924.7	898.8	-	25.9	13	14	16	-	51	55	10	1	8.	87	9.	35	38	44	47	41.	4.	4.	
4	696.5	692.4	-	4.1	1.6	.2	6.4	18	5.1	.7	3.3	1	3	.6	5	5.2	4	0.4	.6	5	5	5	
2	59.6	-	-	-	55.	-	10	14	45	65	71.	1	11	1.	-	-	-	-	-	-	-	-	
Totals	2199.7	200.8	-	132.3	9	8	2.9	.8	4.4	.2	7	0	.6	7	-	-	-	-	-	-	-	-	
Level 58					Roundness										Sphericity								
Size (mm)	Weight (g)	Li mes	Sa nd	Ch ert	0.1	%	0.3	%	0.5	%	0.7	%	0.9	%	0.3	%	0.5	%	0.7	%	0.9	%	
63	-	-	-	-	-	-	-	-	-	-	-	-	-	-	-	-	-	-	-	-	-	-	-
31.5	244.9	217.3	-	27.6	89.	36	11	46	42.	17	-	-	-	47	19	11	47	81.	33	-	-	-	
16	655.5	604.8	-	50.7	86.	13	20	31	23	35	11	1	17	2.	10	25	38	31	48	22.	3.	3.	
8	1445.3	141.4	-	31.4	8	.2	5.5	4	0.7	.2	4.7	8	8	7	66	.1	1.3	4	5.8	.2	4	4	
4	992.1	955	-	1	26	18	41	28	63	43	11	8.	10	0.	10	7.	57	39	72	50	44.	3.	
2	139	-	-	-	5.5	.4	6.3	.8	4.3	.9	9.1	2	.1	7	3	1	3.2	.7	5.4	.2	2	1	
Totals	3476.8	319.1	-	146.8	8	.9	2.1	4	8.8	.5	3	2	7	1	-	-	-	-	-	-	-	-	
Level 59					Roundness										Sphericity								
Size (mm)	Weight (g)	Li me	Sa nd	Ch ert	0.1	%	0.3	%	0.5	%	0.7	%	0.9	%	0.3	%	0.5	%	0.7	%	0.9	%	
63	537.5	537.5	-	-	-	-	-	-	53	10	-	-	-	-	15	28	38	71	-	-	-	-	-
31.5	190	190	-	-	-	-	12.	6.	13	72	39.	2	-	4	.7	3.1	.3	-	-	-	-	-	
16	677.7	583.5	-	94.2	56.	8.	21	31	29	43	11	1	-	-	-	15	78	39.	20	-	-	-	
8	1159.1	113.5	1.1	1	1	3	2.3	.3	7	.8	2.3	7	-	79	11	21	31	27	40	11	1	1	
4	960.8	950.3	-	11	21	18	17	15	58	50	14	1	29	2.	13	11	45	39	47	40	99.	8.	
2	135.9	-	-	-	7.4	.8	8.5	.4	5.2	.5	8.4	3	.6	6	2	.4	4.8	.2	2.7	.8	9	6	
Totals	3661	339.6	1.1	128.3	14	15	0.4	.7	1.1	.3	1.3	6	.2	4	-	-	-	-	-	-	-	-	
Level 60					Roundness										Sphericity								
Size (mm)	Weight (g)	Li me	Sa nd	Ch ert	0.1	%	0.3	%	0.5	%	0.7	%	0.9	%	0.3	%	0.5	%	0.7	%	0.9	%	
63	-	-	-	-	-	-	-	-	-	-	-	-	-	-	-	-	-	-	-	-	-	-	-
31.5	175.8	146.8	-	29	-	-	29	.5	6.8	.5	-	-	-	-	-	-	78.	44	97.	55	-	-	
16	614.7	549.8	-	9	10	16	19	31	26	43	47.	7.	7.	1.	67	10	18	30	31	-	42.	6.	
8	1036.4	100.6	-	5	1	.4	4	.6	5.1	.1	5	7	1	2	.2	.9	5.6	.2	9.5	52	4	9	
4	902.6	887.9	-	9	17	17	16	16	53	51	14	1	12	1.	66	6.	30	29	60	61.	5.	5.	
2	63.4	-	-	-	6.2	17	7.8	.2	2.8	.4	7.4	4	.2	2	.7	4	6.8	.6	1.4	58	5	9	
Totals	2792.9	259.0	-	140.3	7	4	5.5	.2	4.4	.2	4.4	3	.1	2	-	-	-	-	-	-	-	-	

Level 61					Roundness										Sphericity							
Size (mm)	Weight (g)	Li me	Sa nd	Ch ert	0.1	%	0.3	%	0.5	%	0.7	%	0.9	%	0.3	%	0.5	%	0.7	%	0.9	%
63	151.7	151.7	-	-	-	-	15	10	-	-	-	-	-	-	-	-	15	10	-	-	-	-
	644.	589	-	55.	17	26	86.	13	20	31	18	2	-	-	27	42	18	28	18	28	-	-
31.5	5	.2	-	3	0.6	.5	6	.4	1.7	.3	5.6	9	-	-	7	.9	3	.4	4.7	.7	-	-
	1155	102	10.	115	21	18	25	22	46	40	20	1	9.	0.	11	-	33	-	43	37	27	2
16	.5	9	9	.9	7.6	.8	5.4	.1	5.4	.3	7.5	8	6	8	6	10	5.1	29	1.6	.4	2.9	4
	1411	133	-	74.	25	18	23	16	67	47	22	1	13	-	10	7.	37	26	78	55	14	1
8	.3	6	-	9	8.9	.3	4.4	.6	6	.9	8.4	6	.6	1	8	7	2.4	.4	6.7	.7	4.1	0
	781.	761	-	19.	13	16	11	14	39	50	13	1	8.	1.	-	-	-	-	-	-	-	-
4	3	.4	-	9	0.5	.7	4.9	.7	3	.3	4.4	7	6	1	-	-	-	-	-	-	-	-
	83.1	-	-	-	-	-	-	-	-	-	-	-	-	-	-	-	-	-	-	-	-	-
	4227	386	10.		77	18	84	20	17	41	75	1	31	0.								
Totals	.4	7	9	266	7.6	.8	3	.3	36	.9	5.9	8	.8	8								

APPENDIX F

2012 RADIOCARBON DATES

<u>UCIAMS-</u>	<u>SAMPLE TYPE</u>	<u>FIELD NUMBER</u>	<u>STRAT LOCATION</u>	<u>CHEMICAL FRACTION DATED</u>	<u>Fm</u>	<u>FM SD</u>	<u>14C AGE</u>	<u>14C SD</u>
UCIAMS- 120329	CHARCOAL	136-1	Geologic Unit 4	ABA CHARCOAL	0.0608	7.00E- 04	22,490	100
UCIAMS- 120330	CHARCOAL	201-1	Geologic Unit 3	ABA CHARCOAL	0.0379	7.00E- 04	26,290	150
UCIAMS- 120331	CHARCOAL	223-1	Geologic Unit 3	ABA CHARCOAL	0.0111	7.00E- 04	36,120	480
UCIAMS- 121950	CHARCOAL	223-1	Geologic Unit 3	ABA-NITRIC ACID CHARCOAL	0.0105	8.00E- 04	36,590	650
UCIAMS- 120332	CHARCOAL	655-15	Geologic Unit 3/2	ABA CHARCOAL	0.0207	7.00E- 04	31,140	270
UCIAMS- 121951	CHARCOAL	655-15	Geologic Unit 3/2	ABA-NITRIC ACID CHARCOAL	0.0213	8.00E- 04	30,910	320
UCIAMS- 120333	CHARCOAL	388-1	Geologic Unit 2	ABA CHARCOAL	0.0218	7.00E- 04	30,740	240
UCIAMS- 120334	CHARCOAL	609-1	Geologic Unit 2	ABA CHARCOAL	0.0378	7.00E- 04	26,310	150
UCIAMS- 120335	CHARCOAL	341-01	Geologic Unit 1	ABA CHARCOAL	0.0221	6.00E- 04	30,620	240
UCIAMS- 120336	CHARCOAL	512-1	Geologic Unit 1	ABA CHARCOAL	0.0028	0.0174	>26,400	---

APPENDIX G
CORRELATIONS

Duck River			Pomme de Terre River			Douthard Creek		
Stratigraphy	Inferred Dates*	¹⁴ C	Stratigraphy	Inferred Dates*	¹⁴ C	Stratigraphy	Inferred Dates*	¹⁴ C
Sowell Mill Formation	0 - 400	150* 380 ± 35	Pippens Formation	0 -900	190 ± 40 430 ± 100 840 ± 60	Holocene Terrace 2	Modern	
Leftwich Formation	8000-1500	1570 ± 230 2980 ± 600 3860 ± 500 4130 ± 130 7250 ± 350	Rodgers Formation	10,000-1680	1680 ± 100 4585 ± 120 7490 ± 170 8100 ± 140 10,200 ± 330	Holocene Terrace I	10,000-3840	3840 ± 40 6360 ± 40
Cannon Bend Formation	10,000-8000							
Cheek Bend Formation	32,000-14,000	14,860 31,320 ± 1550 32,330 ± 2720	Boney Spring Formation	32,000-13,500	13,550 ± 400 16,580 ± 220 21,380 ± 500 22,730 ± 590 26,440 ± 1,170 30,880 ± 1320 31,880 ± 1340	Douthard Paleosol	30,000-22,000	22490 ± 150